*Algerian People's Democratic Republic*
*Ministry of Higher Education and Scientific Research*
*Larbi Tebessi University - Tebessa*
*Faculty of Exact Sciences and Life Sciences*
*Department: Mathematics and Computer Science*

*Final thesis*
*For the attainment of the MASTER's degree*
*Field: Mathematics and Computer Science*
*Program: Mathematics*
*Option: Partial Differential Equations and Applications*

*Topic:*

# Chaos in some Zeraoulia-Sprott mappings

*Presented by:*
***Khadidja Boughrara***

*In front of the jury:*

| | | | |
|---|---|---|---|
| *Mr, Rebiai Belgacem* | *Prof* | *Université Larbi Tébessi* | *President* |
| *Mr, Hafdallah Abdelhak* | *MCA* | *Université Larbi Tébessi* | *Examiner* |
| *Mr, Elhadj Zeraoulia* | *Prof* | *Université Larbi Tébessi* | *Supervisor* |

*Date of defense: 04/06/2023*

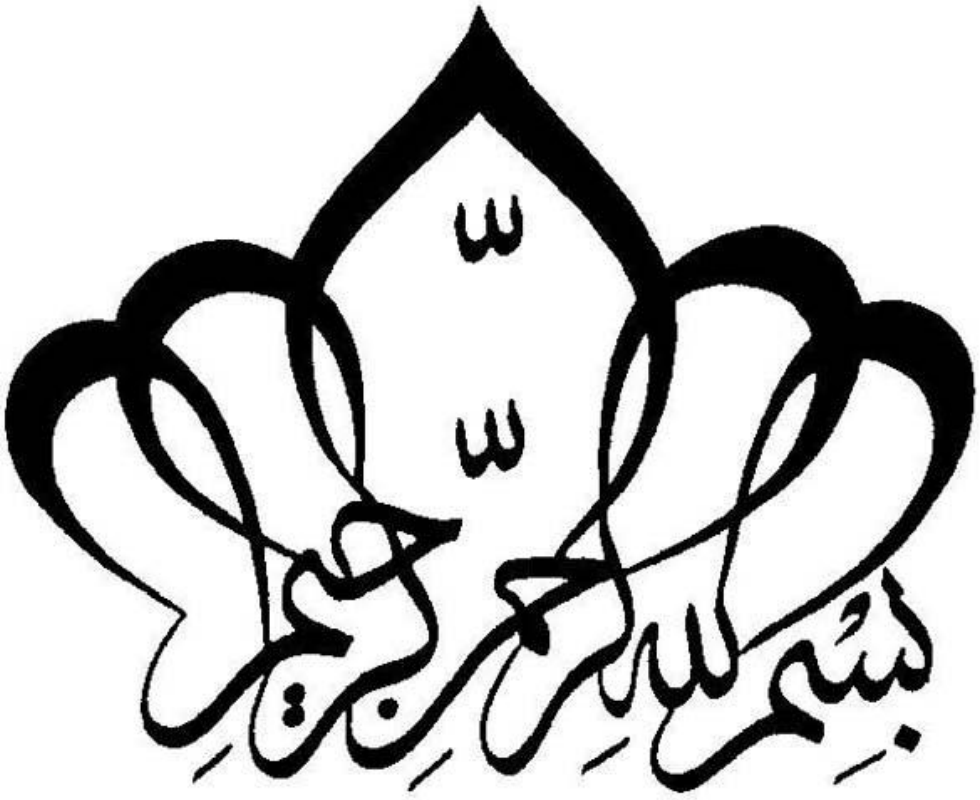
بسم الله الرحمن الرحيم

# شكر و عرفان

الحمد لله الذي منحني القدرة لاتمام هذه المذكرة

بنجاح، أشكر الله عز و جل على النعم العديدة التي منحني

إياها و على القوة و الصبر التي وهبها لي خلال هذه الرحلة التعليمية

أود أن أعبر عن شكري و امتناني لأستاذي المشرف، البروفيسور

الفاضل "زراولية الحاج" الذي وفر لي الدعم و الإرشاد طوال فترة إعداد

المذكرة و قبلها.

لأعضاء هيئة التدريس الكرام شكرًا لكم على العطاء الذي لا ينضب وعلى التفاني والإلهام

الذي قدمتموه لي ولزملائي في الدراسة. أنتم تمثلون القامة العلمية التي نسعى للوصول إليها،

وأنا فخورة بأنني كنت جزءًا من هذه الأسرة التعليمية الرائعة.

أتقدم بخالص الشكر و التقدير لعائلتي و أحبائي الذين وقفوا بجانبي

و دعموني في كل مرحلة من مراحل رحلتي التعليمية.

أسأل الله أن يجعل هذا العمل مقبولا و أن يكون مساهمة صغيرة

في المجال العلمي و يثمر عبير المعرفة و الفهم.

# إهداء

" من قال أنا لها نالها و أنا لها و إن أبت رغما عنها أتيت بها "

إلى نفسي القوية والمثابرة، أنت المحرك والشجاعة وراء هذا الإنجاز. استطعت تجاوز التحديات و الصعوبات، واستمريت في العمل بجد لتحقيق أهدافي. أنت قدوتي وأعتز بك و بالتطور الذي حققته. لا تتوقفي عن التطلع للمزيد وتحقيق ما ترغبين فيه. أنت قوية وملهمة، وأعرف أن لديك مستقبلًا مشرقًا.

إلى الأيادي الطاهرة التي أزالت عن طريقي أشواك الفشل، إلى كل من سندني بكل حب عند ضعفي، إلى من رسمولي المستقبل بخطوط من الثقة و الحب.

أهدي فرحة تخرجي:

إلى تلك الإنسانة العظيمة التي لطالما تمنيت أن تقر عينها برؤيتي في يوم كهذا
" الحبيبة أمي ".
إلى من كلل العرق جبينه و علمني أن النجاح لا يأتي إلا بالصبر و الإصرار
"أبي الغالي".
إلى حبيبة القلب و رفيقة الدرب تلك التي لم و لن تترك يدي طول الطريق
أنت نور في عتمتي " نورة ".
إلى مؤنساتي و رفيقاتي نسائم السعادة دمتم لي شيئًا جميلا لا ينتهي
" مريم، عائشة، آسيا، إكرام "
إلى عبق الفرح و شحنة التفاؤل خالتي و صديقتي و أختي
" سهيلة "
إلى سندي و مصدر القوة و الأمان إخوتي" الحسن، ياسين "

# Abstract

The objective of this thesis is the exploration of chaos in certain **Zeraouilia-Sprott** mappings. In particular, this class of discrete dynamical systems known for their chaotic behaviors.

- In the first chapter, we mentioned some important and comprehensive concepts of dynamical systems theory.
- In the second chapter, we introduced some **Zeraoulia-Sprott** smooth discrete mappings in one and two dimension capable of generating **Chaos**.
- In the third chapter, we studied a simple **2-D** discrete piecewise linear chaotic of **Zeraoulia-Sprott mapping** that is capable of generating a hyperchaotic double scroll attractor.

# Resumé

L'objectif de cette thèse est l'exploration du chaos dans certains modèles de **Zeraouilia-Sprott.** En particulier, cette classe de systèmes dynamiques discrets est reconnue pour son comportement chaotique.

- Dans le premier chapitre, nous avons mentionné certains concepts importants et complets de la théorie des systèmes dynamiques.
- Dans le deuxième chapitre, nous avons introduit certains applications discrets lisses de **Zeraoulia-Sprott** en une et deux dimensions capables de générer du **chaos**.
- Dans le troisième chapitre, nous avons étudié un modèle simple chaotique linéaire en morceaux de **Zeraoulia-Sprott** en 2D, capable de générer un attracteur à double spirale hyperchaotique.

# ملخص


الهدف من هذه الأطروحة هو استكشاف الفوضى في بعض نماذج **زراولية-سبروت.** وعلى وجه الخصوص، هذه الفئة من الأنظمة الديناميكية المتقطعة المعروفة بسلوكها الفوضوي.

- ❖ بالنسبة للفصل الأول، تم ذكر بعض المفاهيم الهامة والشاملة لنظرية النظم الديناميكية.
- ❖ بالنسبة للفصل الثاني، قدمنا بعض تطبيقات توضيحية لنماذج **زراولية-سبروت** للتطبيقات الديناميكية المتسقة في بُعدين، قادرة على توليد الفوضى.
- ❖ بالنسبة للفصل الثالث، قمنا بدراسة نموذج بسيط ثنائي الأبعاد لتطبيق الديناميكي الخطي بالاجزاء ل **زراولية-سبروت،** القادر على توليد جاذب فائق الفوضى.

# Contents

# List of Figures

## Introduction

**Chaos theory** is a crucial branche of the study of dynamical systems. It was coined by the mathematician **Henri Poincaré** at the start of the 20th century while he was working on differential systems, and it has undergone constant development ever since. There are two types of bifurcation: local and global. *Local bifurcation* can be completely explained by changes in the stability of local equilibrium properties, periodic orbits, or other invariant sets as the parameters cross critical thresholds. *Global bifurcation*, on the other hand, frequently happens when the larger invariant sets of the system collide. They cannot be found solely by looking at the security of the equilibriums (fixed points).
In this study, we concentrate on a novel class of bifurcations known as **border collision bifurcations**. When a fixed point (or periodic point) encounters the switching manifold in **piecewise smooth maps**, a bifurcation, which can be classified into two types namely *border collision pair bifurcation* and *border crossing bifurcation*.
We focus on continuous piecewise smooth discrete-time systems in one and two dimensions when studying bifurcation theory. We have divided this master thesis into three chapters as follows:

- **Chapter 1,** is dedicated to presenting the key findings regarding chaotic dynamics and bifurcations in piecewise smooth maps in one and two dimensions.
- **Chapter 2,** is focused only on searching chaos in 1 and 2-dimensional smooth discrete **Zeraoulia- Sprott mappings.**
- **Chapter 3**, is interested in the serching of choas in some two-dimensional piecewise **Zeraoulia-Sprott mappings**.

# Chapter 1

# Border Collision Bifurcations

**The border collision bifurcations** are relativley a new class of bifurcations that are entirely distinct from everything we have previously examined, including saddle node, pitchfork, hopf, etc. It first appeared as a term in [6], though it was previously presented in Russian literature under the name **C-bifurcation** attributed to the scientist Feigen in [5], and it specifically occurs in piecewise smooth maps for the reason that the latter is very effective at accurately modeling the non-smoothness in the systems. Switching circuits are an example of this from physics, as this type of bifurcation is clearly manifested, implies that this bifurcation falls under the category of global bifurcation that results in the so-called **robust chaos** and happens when the fixed point's nature changes as it crosses the switching surface. However, we are only interested in searching a portion of these bifurcations.

## 1.1 Maps and their bifurcation

### 1.1.1 Fixed point and periodic orbits of maps

A discrete time system is defined by a difference equation:

$$x_{n+1} = f_\mu(x_n), \quad x_n \in \mathbb{R}^n, \ \mu \in \mathbb{R}$$

simple solutions include:
**Fixed Points:** $x_{n+1} = x_n$, that is solutions of $x^* = f(x^*)$.
**Periodic Orbits:** $(x_0, \ldots, x_{p-1})$ with $x_k = f(x_{k-1}), k = 1, \ldots, p-1$ and $x_0 = f(x_{p-1})$. Therefore,

$$x_k = f^p(x_k) = \underbrace{f(\cdots(f(x_k))\cdots)}_{p \ iterations}, \quad k = 0, 1, 2, \cdots p-1.$$

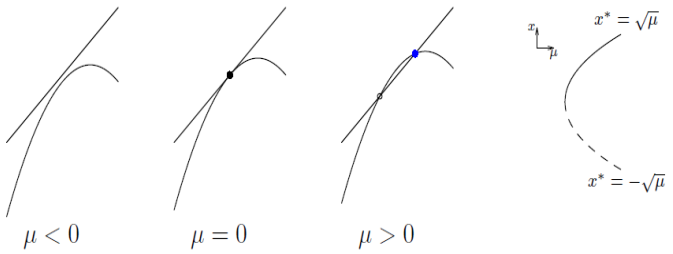


Figure 1.1: Saddle-node (tangential) bifurcation.

That is, periodic points are fixed points of an iterate $f^p$ of the map. The stability of fixed points or periodic orbits can also be studied via linearisation. A fixed point $x^*$ is linearly stable if $|f'(x^*)| < 1$. For the linear stability of a periodic orbit, there is only one condition: $\prod_{k=0}^{p-1} |f'(x_k)| < 1$.

### 1.1.2 Bifurcation of maps

**Saddle-node (tangential) bifurcation**: For $x_{n+1} = \mu + x_n - x_n^2$
If $\mu > 0$, there are two fixed points $x_\pm^* = \pm\mu^{1/2}$; the fixed point $x_+^* = \mu^{1/2}$ is stable but $x_-^* = -\mu^{1/2}$ is not stable.
If $\mu = 0$, there is one fixed point $x^* = 0$, this fixed point is indifferent because $|f'(x^*)| = 1$
If $\mu < 0$, there is no fixed point. Because bifurcation occurs when the straight line $y = x$ touches the parabola $y = \mu + x - x^2$ tangentially at $\mu = 0$, (See Figure 1.1).

**Transcritical bifurcation**: For $x_{n+1} = (1+\mu)\, x_n - x_n^2$
There are always two fixed points $x^* = 0$ and $x^* = \mu$. The fixed point $x^* = 0$ is stable for $\mu < 0$, but becomes unstable for $\mu > 0$, while the other fixed point $x^* = \mu$ is unstable for $\mu < 0$ and stable for $\mu > 0$.

**Supercritical pitchfork bifurcation**: For $x_{n+1} = (1+\mu)\, x_n - x_n^3$
When $\mu < 0$, there is only one fixed point $x^* = 0$, which is stable.
When $\mu > 0$, there are three fixed points; $x^* = \pm\mu^{1/2}$ are stable, but $x^* = 0$ unstable.

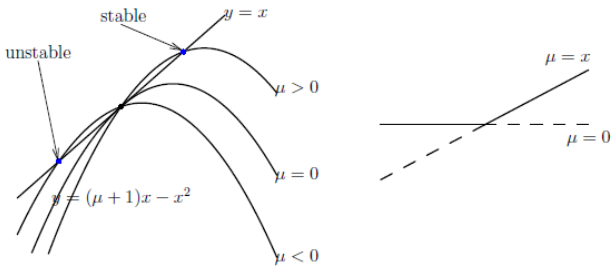


Figure 1.2: Transcritical bifurcation.

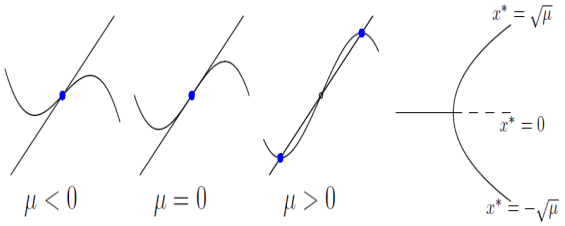


Figure 1.3: Pitchfork bifurcation.

### 1.1.3 Logistic map

The *logistic* map is the simplest quadratic family of maps:

$$f_\mu(x) = \mu x(1-x), \quad \mu \geq 0,$$

In the context of population dynamics, the two terms $\mu x$ and $-\mu x^2$ in this map can be interpreted as reproduction and starvation (density dependent mortality) respectively.

**Fixed points**: There are two fixed points $x^* = 0$ and $x^* = (\mu - 1)/\mu$, provided $\mu \geq 1$.

**Linear stability**: We have that $f'_\mu(x) = \mu - 2x\mu$. If $0 \leq \mu < 1$, the fixed point $x^* = 0$ is stable, and the fixed point $x^* = (\mu - 1)/\mu$ is not in the range $[0, 1]$. If $\mu \geq 1$, the fixed point $x^* = 0$ becomes unstable, but $x^* = (\mu - 1)/\mu$ become stable,as long as $1 < \mu < 3$.Because the fixed points $x^* = 0$ and $x^* = (\mu - 1)/\mu$ exchange stability at $\mu = 1$, this is a transcritical bifurcation.

**Period-doubling bifurcation**: As $\mu$ passes 3, $x^* = (\mu - 1)/\mu$ becomes unstable (see Figure 4). A period-two orbit $(x^*_+, x^*_-)$ appears, such that

$$x^*_+ = f'_\mu(x^*_-), \quad x^*_- = f'_\mu(x^*_+).$$

In other words, both $x^*_+$ and $x^*_-$ are fixed points of $x = f_\mu(f_\mu(x))$, but not fixed points of $x = f_\mu(x)$. It's called *period-doubling bifurcation,* signified by $f'_{\mu^*}(x^*) = -1$ at $\mu^* = 3$.

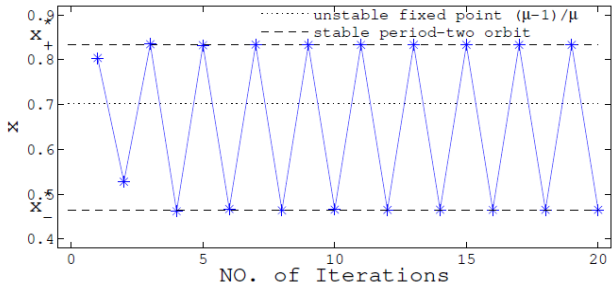


Figure 1.4: The fixed point $x^* = (\mu - 1)/\mu$ becomes unstable as $\mu > 3$, and a period-two orbit emerges (the iteration for $\mu = 3.35$ is plotted here).

Since

$$x - f_\mu(f_\mu(x)) = x(\mu x - \mu + 1)\left(\mu^2 x^2 - (\mu^2 + \mu)x + \mu + 1\right).$$

all fixed points of $x = f_\mu(f_\mu(x))$ are

$$x^* = 0,\ x^* = \frac{\mu - 1}{\mu}, \quad x^*_\pm = \frac{\mu + 1 \pm \sqrt{(\mu - 3)(\mu + 1)}}{2\mu}.$$

The first two are inherited from $x^* = f_\mu(x^*)$ and the last two form the period two orbits.

### 1.1.4 Bifurcation of two-dimensional maps

By observing that when a parameter changes, results in eigenvalues of the Jacobian matrix with unit modulus, the same method may be used to investigate the bifurcation of two-dimensional maps.

**Example 1.1** *Consider the map*

$$x_{n+1} = \mu y_n + x_n - x_n^2, \qquad y_{n+1} = x_n.$$

*There are two fixed points*

$$\begin{aligned}(x_1^*, y_1^*) &= (0, 0),\\ (x_2^*, y_2^*) &= (\mu, \mu).\end{aligned}$$

*The Jacobian matrix*

$$J(x, y) = \begin{pmatrix} 1 - 2x & \mu \\ 1 & 0 \end{pmatrix}.$$

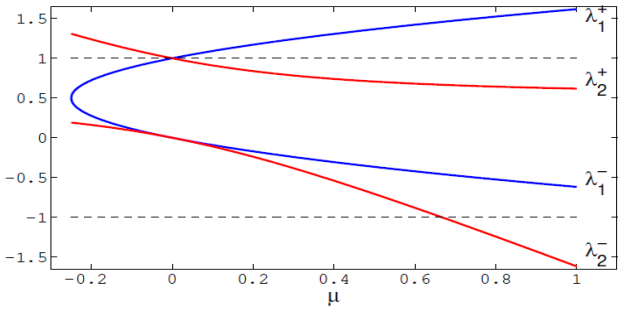


Figure 1.5: The eigenvalues of the Jacobian matrix near the two fixed points $(0,0)$ and $(\mu,\mu)$.

*we get*

$$J(x_1^*, y_1^*) = \begin{pmatrix} 1 & \mu \\ 1 & 0 \end{pmatrix}, \quad J(x_2^*, y_2^*) = \begin{pmatrix} 1-2\mu & \mu \\ 1 & 0 \end{pmatrix}.$$

For the fixed point $(x_1^*, y_1^*)$, the two eigenvalues are governed by

$$\lambda_1^{\pm} = \frac{1 \pm \sqrt{1+4\mu}}{2}$$

For the fixed point $(x_1^*, y_1^*)$, the two eigenvalues are governed by

$$\lambda_2^{\pm} = \frac{1-2\mu \pm \sqrt{1+4\mu^2}}{2}.$$

The stability of the two fixed points $(x_1^*, y_1^*)$ and $(x_2^*, y_2^*)$ are exchanged, indicating the *transcritical bifurcation* at $\mu = 0$. The bifurcation is also clear from Figure 5. The fixed point $(x_1^*, y_1^*) = (0,0)$ is stable, for $\mu \in (-1/4, 0)$. The other fixed point $(x_2^*, y_2^*) = (\mu, \mu)$ is stable for $\mu > 0$, but becomes unstable again when $\lambda_2^- = -1$, or $\mu = 2/3$. A period-doubling bifurcation occurs here (associated with eigenvalue $-1$).

Other concepts: intermittancy, Lyapunov exponent and the route to chaos
Other significant ideas inspired by maps include:

- Complex iterations from fractals (Julia sets).
- Chaos and its characterisation (sensitive dependence on initial data, existence of **strange attractors**, . . . )
- Intermittancy (jumping between nearly periodic and chaotic motions) in chaotic regime.
- Lyaponov exponents (rate of separation of close trajectories).

## 1.2 Piecewise smooth maps

This section examines the piecewise smooth map in one and two dimensions by focusing on three key ideas: the map's definition, some of its characteristics, the normal form and fixed points in both dimensions, and finally the border collision bifurcations. Consider a map $F : \mathbb{R}^m \to \mathbb{R}^m$ as follow:

$$x_{n+1} = F(x_n), \quad x_0 \in \mathbb{R} \tag{1.1}$$

**Some properties**

- The map (1.1) is a piecewise smooth, if the phase space $\mathbb{R}^m$ can be partitioned into a finite number $J$ of disjoint non-empty open regions $R_i$, $i = 1, ..., J$, and a boundary $\Sigma$, so that $\mathbb{R}^m = \left(\bigcup_{i=1}^{J} R_i\right) \cup \Sigma$.
- The boundary $\Sigma$ made up of a union of continuously differentiable surfaces which separate the regions $R_i$.
- $F$ is smooth in each regions $R_i$.
- Non-smoothness of $F$ occurs on $\Sigma$, which is called **switching surface** or switching manifold.
- The map (1.1) is also known as **hybrid system**. For more details see [7].

The most significant findings regarding these maps relate to the relationship between chaotic behaviors and boundary collision bifurcations. Notice that some ingredients form the basis for the study of this relationship. The first of these is *the affinity of the corresponding normal forms* for fixed points on the borders, and the second is *the behavior of fixed points* (or periodic points) depending on the bifurcation parameters associated with the various cases. This study is conducted in one and two dimensions using the following informations, which is taken from [8] and [9]:

### 1.2.1 One-dimensional piecewise smooth maps

Consider the following 1-D piecewise smooth system:

$$x_{n+1} = f\ (x_n, \mu) = \begin{cases} g\,(x, \mu)\,, & x < x_b \\ h\,(x, \mu)\,, & x > x_b \end{cases} \tag{1.2}$$

where $\mu$ is the bifurcation parameter, the smooth curve $x = x_b$, the state space was separated into two regions. $R_L$ and $R_R$ given by:

$$\begin{cases} R_L = \{x \in \mathbb{R} : x < x_b\} \\ R_R = \{x \in \mathbb{R} : x > x_b\} \end{cases}$$

and the boundary between them is given by:

$$\Sigma = \{x \in \mathbb{R} : x = x_b\}$$

**Some properties**

- The map $f$ is continuous, but its derivative is discontinuous at the borderline $x = x_b$.
- The functions $g$ and $h$ are both continuous and they have continuous derivatives in $x$ everywhere except at $x_b$.
- $x_0(\mu)$ is a possible path of fixed points of $f$, this path depends continuously on $\mu$.
- The possible fixed point hits the boundary at a critical parameter value $\mu_b : x_0(\mu_b) = x_b$.

**The normal form**

We need the following theorem in order to simplify and streamline the study of border collision bifurcations in 1-D piecewise smooth maps:

**Theorem 1.1** *The piecewise smooth one-dimensional map (1.2) has the following normal form, which is given by [9]:*

$$N_1(x, \mu) = \begin{cases} ax + \mu, & x < 0 \\ bx + \mu, & x > 0 \end{cases} \tag{1.3}$$

*where $\mu$ is a parameter and $a, b$ are the graph's slopes at its two sides. ($R_L$ and $R_R$) of the border $x = 0$.*

**Proof.** The normal form (1.3) at a fixed point on the border is a piecewise affine approximation of the map in the neighborhood of the border point $x_b$. The method of derivation of such a form is as follows:

1. Let $\bar{x} = x - x_b$ and $\bar{\mu} = \mu - \mu_b$, then the equation (1.2) becomes:

$$\bar{f}\ (\bar{x}, \bar{\mu}) = \begin{cases} g(\bar{x} + x_b, \bar{\mu} + \mu_b), & \bar{x} < 0 \\ h(\bar{x} + x_b, \bar{\mu} + \mu_b), & \bar{x} > 0 \end{cases} \tag{1.4}$$

   Hence, for map (1.4), we have the following properties:

   - The border is at $\bar{x} = 0$.
   - Two halves of the state space are present $\mathbb{R}_- = (-\infty, 0]$ and $\mathbb{R}_+ = [0, \infty)$.
   - The fixed point of (1.4) is at the border for the parameter value $\bar{\mu} = 0$.

2. Expanding $\bar{f}$ to first order about $(0,0)$ gives:

$$\begin{cases} \bar{f}\ (\bar{x},\bar{\mu}) = \begin{cases} a\bar{x}+\bar{\mu}\upsilon+O\left(\bar{x},\bar{\mu}\right), & \bar{x}<0 \\ b\bar{x}+\bar{\mu}\upsilon+O\left(\bar{x},\bar{\mu}\right), & \bar{x}>0 \end{cases} \\ a=\lim_{x\to 0^-}\frac{\partial}{\partial x}\bar{f}\ \ (\bar{x},0) \\ b=\lim_{x\to 0^+}\frac{\partial}{\partial x}\bar{f}\ \ (\bar{x},0) \\ \upsilon=\lim_{x\to 0}\frac{\partial}{\partial \mu}\bar{f}\ \ (\bar{x},0) \end{cases} \tag{1.5}$$

such that:

- Due to the smoothness of $f$ in $\mu$, the last limit in (1.5) doesn't depend on the direction of approach of $0$ by $x$.
- The non-linear terms close to the boundary are negligible under the hypotheses $\upsilon \neq 0, |a| \neq 1$ and $|b| \neq 1$.

3. Finally, we define a new parameter $\mu'' = \bar{\mu}\upsilon$ and dropping the higher order terms as in [2], then the 1-D normal form is given by:

$$G_1\left(x,\bar{\mu}\right) = \begin{cases} a\bar{x}+\mu'', & \bar{x}<0 \\ b\bar{x}+\mu'', & \bar{x}>0 \end{cases}$$

It is similar to the form in (1.3).

■

**The fixed points**

- To the right $(x > x_b)$ and left $(x < x_b)$, respectively, of the boundary, let $x_R^*$ and $x_L^*$ be the system's possible fixed points. Then in the normal form (1.3) we have

$$\begin{cases} x_R^* = \frac{\mu}{1-b} > 0, \ \text{ if } \ b<1 \wedge \mu>0 \\ \text{and} \\ x_L^* = \frac{\mu}{1-a} < 0, \ \text{ if } \ a<1 \wedge \mu<0 \end{cases}$$

**Border collision bifurcation scenarios:** Now, we go over a few border collision bifurcation scenarios from $x_b$ with $\mu$ close to $\mu_b$.

- **Border collision bifurcation scenarios** can be obtained by various combinations of the parameters $a \geq b$ as $\mu$ is varied. It is the same for $a < b$ which are summarized in Figure 1.6, because the normal form (1.3) is invariant under the transformation $x \to -x$, $\mu \to -\mu$, $a \rightleftarrows b$. See also [9]:

**Scenario 1:** *(Persistence of stable fixed point) or Period-1 → Period-1*.

If $-1 < b \leq a < 1$, then there is no bifurcation and a stable fixed point for $\mu < 0$ persists and remains stable for $\mu > 0$.

**Scenario 2:** *(Persistence of unstable fixed point) or No Attractor → No Attractor*.

If $1 < b \leq a$ or $b \leq a < -1$, then there is no bifurcation and an unstable fixed point for $\mu < 0$ persists and remains unstable for $\mu > 0$.

**Scenario 3:** *(Merging and annihilation of stable and unstable fixed points) or No Fixed Point → Period-1*.

If $-1 < b < 1 < a$, then there is a bifurcation from no fixed point for $\mu < 0$ to two fixed points $x_L$ (unstable) and $x_R$ (stable) for $\mu > 0$.

**Scenario 4:** *(Merging and annihilation of two unstable fixed points, plus chaos). No fixed point → chaos*.

If $a > 1$ and $\frac{-a}{a-1} < b < -1$, then there is a bifurcation from no fixed point to two unstable fixed points plus a growing chaotic attractor as $\mu$ is increased through zero.

**Scenario 5:** *(Merging and annihilation of two unstable fixed points) or No fixed point → No attractor*.

If $a > 1$ and $b < \frac{-a}{a-1}$, then there is a bifurcation from no fixed point to two unstable fixed points as $\mu$ is increased through zero and there is an unstable chaotic orbit for $\mu > 0$.

**Scenario 6:** *(Supercritical border collision period doubling) or Period-1 → Period-2*.

If $b < -1 < a < 0$ and $-1 < ab < 1$, then there is a bifurcation from a stable fixed point $x_L$ to an unstable fixed point $x_R$ plus a stable period-2 orbit as $\mu$ is increased through zero.

**Scenario 7:** *(Subcritical border collision period doubling) or Period-1 → No Attractor*.

If $b < -1 < a < 0$ and $ab > 1$, then there is a bifurcation from a stable fixed point $x_L$ plus an unstable period-2 orbit to an unstable fixed point $x_R$ as $\mu$ is increased though zero.

**Scenario 8:** *(Emergence of periodic or chaotic attractor from stable fixed point) or Period-1 → Periodic or Chaotic Attractor.*

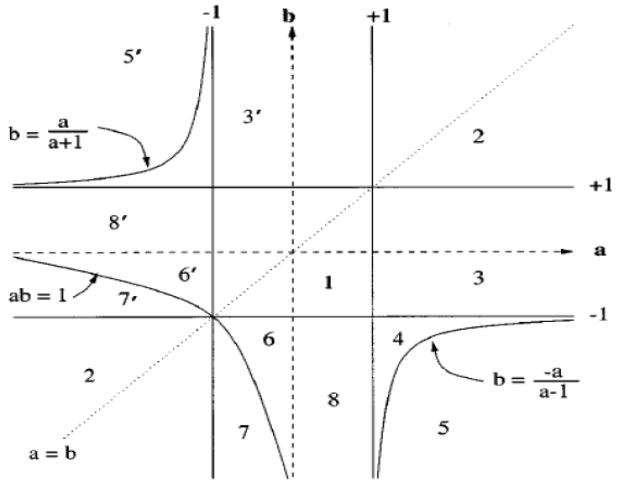


Figure 1.6: Partitioning of the parameter space into regions with the same qualitative phenomena. The labeling of regions refers to various bifurcation scenarios. 1) *Persistence of stable fixed points,* 2) *Persistence of unstable fixed points*, 3) *No fixed point to stable and unstable fixed points,* 4) *No fixed point to two unstable fixed points and chaotic attractor*, 5) *No fixed point to two unstable fixed points,* 6) *Supercritical border collision period doubling,* 7) *Subcritical border collision period doubling,* 8) *A stable fixed point to periodic or chaotic attractor*. The regions shown in primed numbers have the same bifurcation behavior as the unprimed ones when $\mu$ is varied in the opposite direction.

If $0 < a < 1$, $b < -1$ and $ab < -1$, then there is a bifurcation from a stable fixed point $x_L$ to an unstable fixed point $x_R$ plus a period-$n$ attractor, $n \geq 2$ or a chaotic attractor which is depends on the pair of parameters $(a, b)$ as shown in Figure 1.7 as $\mu$ is increased through zero.

- Now we give the following definitions. For more details see [10]:

**Definition 1.1** *The border collision pair bifurcation is a kind of border collision bifurcations and its similar to saddle node bifurcation (or tangent bifurcation) in smooth systems, The smooth map in this bifurcation has no fixed points for negative (respectively, positive) values of $\mu$, and two fixed points for positive (respectively, negative) values of $\mu$ (one fixed point on one side of the border and the other fixed point on the other side). Consequently, the border collision pair bifurcation occurs if:*

$$b < 1 < a$$

**Definition 1.2** *The border crossing bifurcation, a kind of border collision bifurcation, resembles smooth maps' period doubling bifurcation in several ways (supercritical period doubling bifurcation*

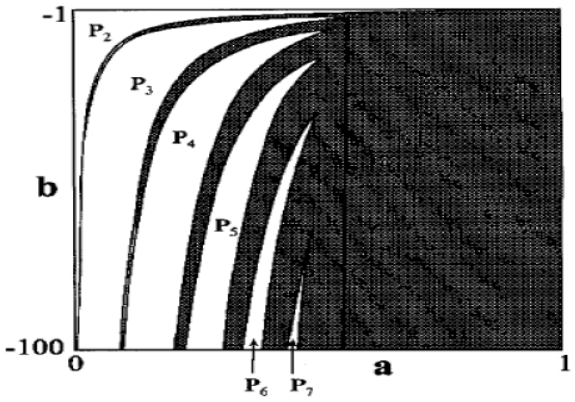


Figure 1.7: The parameter region $0 < a < 1$ and $b < -1$, showing the type of attractor for $\mu > 0$. Regions $P_n$ correspond the existence of stable period $n$ orbit, inside the shaded region there exists chaotic attractors.

*in smooth maps with one distinction). In this bifurcation, the fixed point remains and crosses the boundary as $\mu$ varies through zero and as additional attractors or repellers emerge or vanish as a result of the split. In fact, border crossing bifurcation happens if*

$$a > -1 \ \text{ and } \ b < -1$$

**Remark 1.1** *We may summarize these particular scenarios as follows in light of the previous definitions:*

- *The two scenarios 1 and 2 belongs to the* ***Scenario A*** *"Persistence of stable fixed point", at $\mu = 0$.*
- *The three scenarios 3, 4 and 5 belongs to the* ***Scenario B*** *"Border collision pair bifurcation".*
- *The last three scenarios 6, 7 and 8 belongs to the* ***Scenario C*** *"Border crossing bifurcation".*

### 1.2.2 Two-dimensional piecewise smooth maps

Let us consider the following 2-D piecewise smooth system given by:

$$g(\hat{x}, \hat{y}, \rho) = \begin{pmatrix} g_1 = \begin{pmatrix} f_1(\hat{x}, \hat{y}, \rho) \\ f_2(\hat{x}, \hat{y}, \rho) \end{pmatrix}, & \text{if } \ \hat{x} < S(\hat{y}, \rho) \\ g_2 = \begin{pmatrix} f_3(\hat{x}, \hat{y}, \rho) \\ f_4(\hat{x}, \hat{y}, \rho) \end{pmatrix}, & \text{if } \ \hat{x} > S(\hat{y}, \rho) \end{pmatrix} \tag{1.6}$$

where $\rho$ is the bifurcation parameter, the smooth curve $\hat{x} = S(\hat{y}, \rho)$ created two regions in the phase plane $R_L$ and $R_R$ given by:

$$\begin{cases} R_L = \{(\hat{x}, \hat{y}) \in \mathbb{R}^2, \ \ \hat{x} < S(\hat{y}, \rho)\} \\ R_R = \{(\hat{x}, \hat{y}) \in \mathbb{R}^2, \ \ \hat{x} > S(\hat{y}, \rho)\} \end{cases}$$

and the boundary between them as:

$$\Sigma = \left\{(\hat{x}, \hat{y}) \in \mathbb{R}^2, \ \ \hat{x} = S(\hat{y}, \rho)\right\}$$

***Some properties***

- Although the map $g$ is continuous, its derivation discontinues at the borderline $\hat{x} = S(\hat{y}, \rho)$.
- Both $g_1$ and $g_2$ are continuous functions with continuous derivatives.
- In each subregion $R_L$ and $R_R$, the one-sided partial derivatives near the boundary are finite.
- The map (1.6) has one fixed point in $R_L$ and one fixed point in $R_R$ for a value $\rho_*$ of the parameter $\rho$.

**The normal form**

As demonstrated in [9], the findings presented above in 1-D normal form provide a complete description of the bifurcations as $\mu$ is varied. For 2-D piecewise smooth maps, the normal form for border collision bifurcation may once more be stated as demonstrated in [8] as follows:

**Theorem 1.2** *The piecewise smooth two-dimensional map (1.6) has the following normal form:*

$$N_2(x, y) = \begin{cases} \begin{pmatrix} \tau_L & 1 \\ -\delta_L & 0 \end{pmatrix} \begin{pmatrix} x \\ y \end{pmatrix} + \begin{pmatrix} 1 \\ 0 \end{pmatrix} \mu, & x < 0 \\ \begin{pmatrix} \tau_R & 1 \\ -\delta_R & 0 \end{pmatrix} \begin{pmatrix} x \\ y \end{pmatrix} + \begin{pmatrix} 1 \\ 0 \end{pmatrix} \mu, & x > 0 \end{cases} \tag{1.7}$$

*where $\mu$ is a parameter and $\tau_{L,R}$ , $\delta_{L,R}$ are the traces and determinants of the corresponding matrices of the linearized map in the two subregions $R_L$ and $R_R$.*

**Proof.** The normal form (1.7) at a fixed point on the border is a piecewise affine approximation of the map in the neighborhood of the borderline $\hat{x} = S(\hat{y}, \rho)$.

- The method of derivation of such a form is as follows:

1. Let $\tilde{x} = \hat{x} - S(\hat{y}, \rho)$ and $\tilde{y} = \hat{y}$, this $\rho$-dependent change of variables moves the border to the $\tilde{y}$-axis, then the equation (1.6) becomes:

$$g(\tilde{x} + S(\hat{y}, \rho), \hat{y}, \rho) = f\ (\tilde{x}, \tilde{y}, \rho) \tag{1.8}$$

   Hence, for the map (1.8), we have the following properties:

   - The border is $\tilde{x} = 0$.
   - The phase space is divided into two halves $L$ and $R$ (for left and right), by the next transformation of coordinates.
   - The map (1.8) has a fixed point $P_* = (0, \tilde{y}_*(\rho_*))$ on the border when $\rho = \rho_*$.

2. The following steps are a summary of coordinate transformation:

   - Let $e_1$ be a tangent vector in the $\tilde{y}$ direction and suppose that the vector $e_1$ maps to a vector $e_2$.
   - Assume $e_2$ is not parallel to $e_1$.
   - Define new coordinates again as shown in Figure 1.8.
   - Choose the point $P_*$ as the new origin for $e_1$ in the $\bar{y}$ direction and $e_2$ in the $\bar{x}$ direction.
   - In $\bar{x} - \bar{y}$ coordinates, the fixed point $P_*$ is now $(0, 0)$ and the border is given by $\bar{x} = 0$.
   - Define the new parameter $\bar{\mu} = \rho - \rho_*$, so $\bar{\mu}_* = 0$.
   - Rescale $\bar{x}$ and $\bar{y}$ again such that at $\bar{\mu} = 0$ a unit vector along the $\bar{y}$-axis maps to a unit vector along the $\bar{x}$-axis. Then, the map $f(\tilde{x}, \tilde{y}, \rho)$ can be written as $F(\bar{x}, \bar{y}, \bar{\mu})$.

3. Now, write the map $F(\bar{x}, \bar{y}, \bar{\mu})$ in the side $L$ in the matrix form as:

$$F_L(\bar{x}, \bar{y}, \bar{\mu}) = \begin{pmatrix} f_1(\bar{x}, \bar{y}, \bar{\mu}) \\ f_2(\bar{x}, \bar{y}, \bar{\mu}) \end{pmatrix}, \quad \text{and} \quad F_L(0, 0, 0) = \begin{pmatrix} 0 \\ 0 \end{pmatrix}$$

   and linearizing $F(\bar{x}, \bar{y}, \bar{\mu})$ in the neighbourhood of $(0, 0, 0)$, we have

$$F_L(\bar{x}, \bar{y}, \bar{\mu}) = \begin{pmatrix} J_{11} & J_{12} \\ J_{21} & J_{22} \end{pmatrix} \begin{pmatrix} \bar{x} \\ \bar{y} \end{pmatrix} + \bar{\mu} \begin{pmatrix} \upsilon_{Lx} \\ \upsilon_{Ly} \end{pmatrix} + O(\bar{x}, \bar{y}, \bar{\mu}) \quad \text{for } \bar{x} < 0 \tag{1.9}$$

where

$$\begin{cases} J_{11} = \lim\limits_{\bar{x}\to 0^-,\bar{y}\to 0} \frac{\partial}{\partial \bar{x}} f_1(\bar{x},\bar{y},0) \\ J_{12} = \lim\limits_{\bar{x}\to 0^-,\bar{y}\to 0} \frac{\partial}{\partial \bar{y}} f_1(\bar{x},\bar{y},0) \\ J_{21} = \lim\limits_{\bar{x}\to 0^-,\bar{y}\to 0} \frac{\partial}{\partial \bar{x}} f_2(\bar{x},\bar{y},0) \\ J_{22} = \lim\limits_{\bar{x}\to 0^-,\bar{y}\to 0} \frac{\partial}{\partial \bar{y}} f_2(\bar{x},\bar{y},0) \\ v_{Lx} = \lim\limits_{\bar{x}\to 0^-,\bar{y}\to 0} \frac{\partial}{\partial \bar{\mu}} f_1(\bar{x},\bar{y},0) \\ v_{Ly} = \lim\limits_{\bar{x}\to 0^-,\bar{y}\to 0} \frac{\partial}{\partial \bar{\mu}} f_2(\bar{x},\bar{y},0) \end{cases}$$

Then, the equation (1.9) becomes:

$$F_L(\bar{x},\bar{y},\bar{\mu}) = \begin{pmatrix} \tau_L & 1 \\ -\delta_L & 0 \end{pmatrix} \begin{pmatrix} \bar{x} \\ \bar{y} \end{pmatrix} + \bar{\mu} \begin{pmatrix} v_{Lx} \\ v_{Ly} \end{pmatrix} + O\left(\bar{x},\bar{y},\bar{\mu}\right) \quad \text{for} \quad \bar{x} < 0$$

such that

$$J_{11} = \tau_L \text{ (trace)} \quad \text{and} \quad J_{21} = -\delta_L \text{ (determinant)}$$

and since a unit vector along the $\bar{y}$ axis maps to a unit vector along the $\bar{x}$ axis at $\bar{\mu} = 0$, we have

$$J_{12} = 1 \quad \text{and} \quad J_{22} = 0$$

Similarly, for side $R$ we obtain:

$$F_R(\bar{x},\bar{y},\bar{\mu}) = \begin{pmatrix} \tau_R & 1 \\ -\delta_R & 0 \end{pmatrix} \begin{pmatrix} \bar{x} \\ \bar{y} \end{pmatrix} + \bar{\mu} \begin{pmatrix} v_{Rx} \\ v_{Ry} \end{pmatrix} + O\left(\bar{x},\bar{y},\bar{\mu}\right) \quad \text{for} \quad \bar{x} > 0$$

Continuity of the map implies:

$$\begin{pmatrix} v_{Lx} \\ v_{Ly} \end{pmatrix} = \begin{pmatrix} v_{Rx} \\ v_{Ry} \end{pmatrix} = \begin{pmatrix} v_x \\ v_y \end{pmatrix}$$

4. Make another change of variables as follow: Let $x = \bar{x}$, $y = \bar{y} - \bar{\mu} v_y$, and $\mu = \bar{\mu}(v_x + v_y)$ with $(v_x + v_y) \neq 0$. The choice of axis is independent of the parameter. Then, we have the normal form:

$$N(x,y) = \begin{cases} \begin{pmatrix} \tau_L & 1 \\ -\delta_L & 0 \end{pmatrix} \begin{pmatrix} x \\ y \end{pmatrix} + \begin{pmatrix} 1 \\ 0 \end{pmatrix} \mu, & x < 0 \\ \begin{pmatrix} \tau_R & 1 \\ -\delta_R & 0 \end{pmatrix} \begin{pmatrix} x \\ y \end{pmatrix} + \begin{pmatrix} 1 \\ 0 \end{pmatrix} \mu, & x > 0 \end{cases} \tag{1.10}$$

where $\mu$ is the parameter and $\tau_{L,R}\,, \delta_{L,R}$ are the traces and determinants of the corresponding matrices of the linearized map in the two subregions $R_L$ and $R_R$ given by:

$$\begin{cases} R_L = \{(x,y) \in \mathbb{R}^2\}\,, & x > 0 \\ R_R = \{(x,y) \in \mathbb{R}^2\}\,, & x > 0 \end{cases}$$

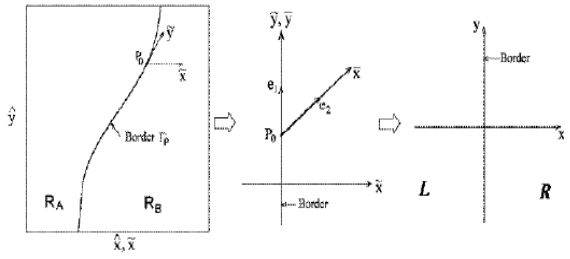


Figure 1.8: The transformation of coordinates from the two-dimensional piecewise smooth map to the normal form.

in the regions $R_L$ and $R_R$, the map (1.10) is smooth and the boundary between them is given by:

$$\Sigma = \{(x, y) \in \mathbb{R}^2, \quad x = 0, \quad y \in \mathbb{R}\}$$

■

**Remark 1.2** *There exists a relation between the piecewise smooth one-dimensional map's normal form and the piecewise smooth two-dimensional map's normal form, where we can move from* $(1.7)$ *to* $(1.3)$ *when* $\delta_i$ *are zero for* $i = L, R$.

**The fixed points:**

- Let $P_L$ and $P_R$ be the possible fixed points of the system near the border to the right: $x < S(\hat{y}, \rho)$ and left: $x > S(\hat{y}, \rho)$ of the border respectively. Then in the normal form (1.7) we have

$$\begin{cases} P_L = \left(\frac{\mu}{1-\tau_L+\delta_L}, \frac{-\delta_L\mu}{1-\tau_L+\delta_L}\right) \in R_L \\ P_R = \left(\frac{\mu}{1-\tau_R+\delta_R}, \frac{-\delta_R\mu}{1-\tau_R+\delta_R}\right) \in R_R \end{cases}$$

  with eigenvalues $\lambda_{L\,1.2}$ and $\lambda_{R\,1.2}$ respectively.

- The eigenvalues of the related Jacobian matrix determine the stability of the fixed points, i.e.,

$$\lambda = \frac{1}{2}\left(\tau \pm \sqrt{\tau^2 - 4\delta}\right)$$

**Border collision bifurcations:** The border collision bifurcations can be obtained by various combinations of the values $\tau_L, \tau_R, \delta_L$ and $\delta_R$ as $\mu$ is varied through zero and because our study of this bifurcations in this dimension is limited only to a part that is the classification of fixed points under the both conditions $|\delta_L| < 1$ and $|\delta_R| < 1$.As a result, the following are the possible fixed point types for the normal form map (1.7) in Figure 1.9:

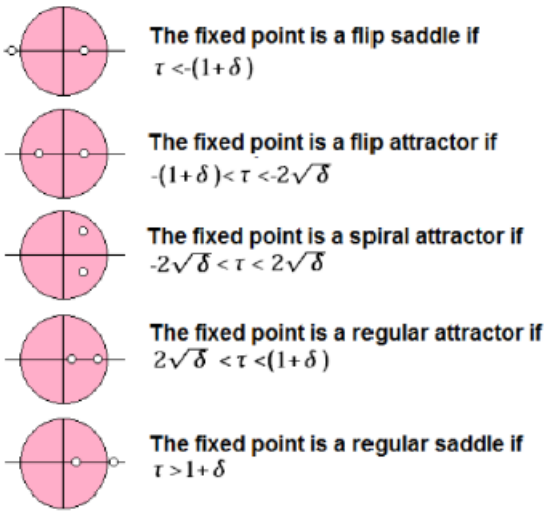


Figure 1.9: The types of fixed points of the normal form map.

**(1)** ***For positive determinant***

**(1.a)** For $2\sqrt{\delta} < \tau < (1+\delta)$, then the Jacobian matrix has two real eigenvalues $0 < \lambda_{1L}, \lambda_{2L} < 1$ and the fixed point is a **regular attractor**.

**(1.b)** For $\tau > 1+\delta$, then the Jacobian matrix has two real eigenvalues $0 < \lambda_{1L} < 1$, $\lambda_{2L} > 1$ and the fixed point is a **regular saddle**.

**(1.c)** For $-(1+\delta) < \tau < -2\sqrt{\delta}$, then the Jacobian matrix has two real eigenvalues $-1 < \lambda_{1L}, \lambda_{2L} < 0$ and the fixed point is a **flip attractor**.

**(1.d)** For $\tau < -(1+\delta)$, then the Jacobian matrix has two real eigenvalues $-1 < \lambda_{1L} < 0$, $\lambda_{2L} < -1$ and the fixed point is a **flip saddle**.

**(1.e)** For $0 < \tau < 2\sqrt{\delta}$, then the Jacobian matrix has two complex eigenvalues $|\lambda_{1L}|, |\lambda_{2L}| < 1$ and the fixed point is a **clockwise spiral**.

**(1.g)** For $-2\sqrt{\delta} < \tau < 0$, then the Jacobian matrix has two complex eigenvalues $|\lambda_{1L}|, |\lambda_{2L}| < 1$ and the fixed point is a **counter-clockwise spiral**.

**(2)** ***For negative determinant***

**(2.a)** For $-(1+\delta) < \tau < (1+\delta)$, then the Jacobian matrix has two real eigenvalues $-1 < \lambda_{1L} < 0, 0 < \lambda_{2L} < 1$ and the fixed point is a **flip attractor**.

**(2.b)** For $\tau > (1+\delta)$, then the Jacobian matrix has two real eigenvalues $\lambda_{1L} > 1, -1 < \lambda_{2L} < 0$ and the fixed point is a **flip saddle**.

**(2.c)** For $\tau < -(1+\delta)$, then the Jacobian matrix has two real eigenvalues $0 < \lambda_{1L} < 1, \lambda_{2L} < -1$ and the fixed point is a **flip saddle**. See also [10].

# Chapter 2

# Chaos in some smooth Zeraoulia-Sprott discrete mappings

This chapter presents some smooth Zeraoulia-Sprott discrete mappings in one and two dimensional with rigorous analysis and numerical simulations along some graphical representation. The presence of chaotic behavior is characterized by sensitive dependence on initial conditions, the emergence of strange attractors, and irregular dynamics. The influence of key parameters on the chaotic dynamics is examined, revealing bifurcations phenomena and transitions between different dynamical regimes that contribute to the understanding of chaos theory in smooth discrete mappings.

## 2.1 Chaos in $S$-unimodality and Collet-Eckmann maps

This section is focused only in 1-D discrete mappings generates chaos.

### 2.1.1 $S$-unimodality

**Definition 2.1** *A map $f : [a, b] \to [a, b]$ is $S$-unimodal on the interval $[a, b]$ if:*

**(a)** The function $f(x)$ is of class $C^3$.

**(b)** The point $a$ is a fixed point with $b$ its other preimage i.e. $f(a) = f(b) = a$.

**(c)** There is a unique maximum at $c \in (a, b)$ such that $f(x)$ is strictly increasing on $x \in [a, c)$ and strictly decreasing on $(c, b]$.

**(d)** The function $f$ has a negative **Shwarzian derivative**, i.e.,

$$S(f,x)=\frac{f'''(x)}{f'(x)}-\frac{3}{2}\left(\frac{f''(x)}{f'(x)}\right)^{2}<0$$

for all $x\in I-\left\{y,f'(y)=0\right\}$.

**Remark 2.1** *The $S$-unimodal mappings have importance in chaos theory due to the theorem given in [11] claiming that each attracting periodic orbit attracts at least one critical point or boundary point. Thus, an $S$-unimodal map can have at most one periodic attractor which will attract the critical point.*

**Theorem 2.1** *Let $f:I\rightarrow I$ be an $S$-unimodal map on the interval $I=[a,b]$, then each attracting periodic orbit attracts at least one critical point or boundary point. Furthermore, each neutral periodic orbit is attracting.*

**Theorem 2.2** *Let $\varphi_{\nu}(x):I=[a,b]\rightarrow I$ be a parametric $S$-unimodal map with the unique maximum at $c\in(a,b)$ and $\varphi_{\nu}(c)=b$, $\forall\nu\in(\nu_{\min},\nu_{\max})$, then $\varphi_{\nu}(x)$ generates robust chaos for $\nu\in(\nu_{\min},\nu_{\max})$. Here $\nu_{\min}$ and $\nu_{\max}$ are defined to be the minimum and the maximum values of the parameter $\nu$ in which $\varphi_{\nu}(x)$ generates robust chaos.*

Let $a<b$ be two real numbers. Let us consider a function $g_{\nu}:[a,b]\rightarrow\mathbb{R}$ and $g_{\nu}$ is of class $C^{3}$. Consider the controlled 1-D discrete mapping given by:

$$\begin{aligned}x_{k+1}&=g_{\nu}(x_{k})+u(x_{k})=\varphi_{\nu}(x_{k}),\\ \nu&\in(\nu_{\min},\nu_{\max}).\end{aligned}\tag{2.1}$$

where $u:[a,b]\rightarrow[a,b]$ is the unknown controller to be chosen. Define the controller $u:[a,b]\rightarrow[a,b]$ by the following conditios:

**(A1)** The controller $u(x)$ is of class $C^{3}$.

**(A2)** The controller $u(x)$ has the following special values:

$$\begin{cases}u(a)=a-g_{\nu}(a)\\ u(b)=a-g_{\nu}(b)\\ \text{There exist a point } c\in(a,b):u'(c)=-g'_{\nu}(c)\end{cases}$$

**(A3)**

$$a - g_\nu(x) \leq u(x) \leq b - g_\nu(x) \quad \text{for all} \quad x \in [a,b].$$

**(A4)**

$$u'(x) > -g_\nu'(x) \quad \text{for all} \quad x \in [a,c).$$

**(A5)**

$$u'(x) < -g_\nu'(x) \quad \text{for all} \quad x \in (c,b].$$

**(A6)**

$$2\left(g_\nu'(x) + u'(x)\right)\left(g_\nu'''(x) + u'''(x)\right) - 3\left(g_\nu''(x) + u''(x)\right)^2 < 0 \text{ for all } x \in [a,b].$$

**Theorem 2.3** *The controlled map (2.1) generates chaos for all* $\nu \in (\nu_{\min}, \nu_{\max})$.

For more informations see [1].

**Proposition 2.1** *The set of controllers* $u$ *verifying conditions* $(A1)$-$(A6)$ *is not empty.*

**Proof.** Take $g_\nu(x) = \upsilon x$, with $x \in [0,1]$ and $\upsilon \in [0,4]$. Define the controller $u(x) = -\upsilon x^2$. Hence, $\varphi_\nu(x) = \upsilon x(1-x)$. The conditions (A1)-(A6) for the controller $u$ are satisfied.
More generally, take $g_\nu(x) = \upsilon x$, with $x \in [0,1]$. Define the controller

$$u(x) = -(\upsilon + \beta + \gamma)x^3 + \beta x^2 + \gamma x,$$

where

$$\begin{cases} 0 \leq \upsilon < \frac{1}{2}, \\ 0 \leq \upsilon < \gamma < 1 - \upsilon, \\ \upsilon + \beta + \gamma < 1, \\ \beta < \min\left\{1 - (\gamma + \upsilon), \frac{1}{6}\sqrt{13\upsilon^2 + 30\upsilon\gamma + 21\gamma^2} - \frac{1}{2}\gamma - \frac{5}{6}\upsilon\right\}. \end{cases}$$

Hence,

$$\varphi_\nu(x) = (-\upsilon - \beta - \gamma)x^3 + \beta x^2 + (\upsilon + \gamma)x.$$

The conditions (A1)-(A6) are satisfied. For the one- dimensional map $\varphi_\nu(x) = \upsilon x(1-x)$, there is only one Lyaponov exponent, defined by

$$LE = \lim_{n\to\infty} \frac{1}{n} \sum_{i=0}^{n-1} \log\left|(2x_i - 1)\upsilon\right|.$$

The Lyaponov exponent is presented in Figure 2.1. Clearly it is strictly positive in a wide range of the bifurcation parameter $\upsilon$. ■

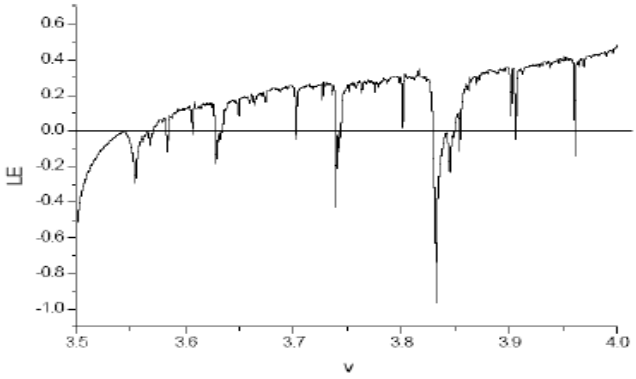


Figure 2.1: The Lyaponov exponent of the map $\varphi_{\nu}(x) = \upsilon x(1-x)$ for $\upsilon \in [3.5, 4]$.

### 2.1.2 Collet-Eckmann condition

Examples of maps characterized by a positive Lyaponov exponent for the critical value are the Collet-Eckmann maps

**Definition 2.2** *A $S$-inimodal maps $f$ is called Collet-Eckmann (CE) if there exist constants $C > 0$, $\lambda > 1$ such that for every $n > 0$ we have that*

$$|D(f^n)(f(c))| > C\lambda^n$$

*where $c$ is the unique critical point of $f$, i.e. $f'(c) = 0$. The unimodal Collet-Eckmann maps are strongly hyperbolic along the critical orbit, i.e., the Collet-Eckmann Condition implies a positive Lyaponov exponent of the system.*

**Definition 2.3** *An analytic family $\{f_\lambda\}$ of unimodal maps is nontrivial if regular if regular parameters are dense.*

**Theorem 2.4** *Let $\{f_\lambda\}$ be a nontrivial analytic family of unimodal maps (in any number of parameters). Then almost every nonregular parameter is Collet-Eckmann.*

Let us consider the controlled 1-D mapings by (2.1) where $u : [a, b] \to [a, b]$ is the unknown controller to be chosen such that: there exist constants $C > 0$, $\lambda > 1$ such that for every $n > 0$ we have that

$$|D((u + g_\nu)^n)((u + g_\nu)(c))| > C\lambda^n.$$

where $c$ is the unique critical point of $\varphi_\nu = u + g_\nu$, i.e. $(u + g_\nu)'(c) = 0$. Define the controller $u : [a, b] \to [a, b]$ by the following conditions:

**(B1)** There exists an invertible function $\xi : [a,b] \to [a,b]$ such that

$$(\xi \circ \varphi_\nu)(x) = (f_\lambda \circ \xi)(x)$$

for all $x \in [a,b]$, where $\{f_\lambda\}$ is any nontrivial analytic family of unimodal maps.

**(B2)** The controller $u(x)$ is of class $C^3$.

**(B3)** The controller $u(x)$ has the following special values:

$$\begin{cases} u(a) = a - g_\nu(a) \\ u(b) = a - g_\nu(b) \\ \text{There exist a point } c \in (a,b) : u'(c) = -g_\nu'(c) \end{cases}$$

**(B4)**

$$a - g_\nu(x) \leq u(x) \leq b - g_\nu(x) \text{ for all } x \in [a,b].$$

**(B5)**

$$u'(x) > -g_\nu'(x) \text{ for all } x \in [a,c).$$

**(B6)**

$$u'(x) < -g_\nu'(x) \text{ for all } x \in (c,b].$$

**(B7)**

$$\begin{aligned} 2\left(g_\nu'(x) + u'(x)\right)\left(g_\nu'''(x) + u'''(x)\right) - 3\left(g_\nu''(x) + u''(x)\right)^2 &< 0 \\ \text{for all } x &\in [a,b]. \end{aligned}$$

**Theorem 2.5** *The controlled map (2.1) generates chaos for almost every nonregular parameter $\lambda$.*

**Proposition 2.2** *The set of controllers $u$ verifying conditions $(B1) - (B7)$ is not empty.*

**Proof.** The quadratic family

$$f_\lambda(x) = \lambda\left(1 - x^2\right) - 1, \qquad \frac{1}{2} \leq \lambda \leq 2$$

is an unimodal map on the interval $[-1,1]$. Let us consider $a, b \in [-1,1]$ such that $-1 < a < b < 1$. Let

$$\xi(x) = \frac{2}{b-a}x + \frac{a+b}{a-b}$$

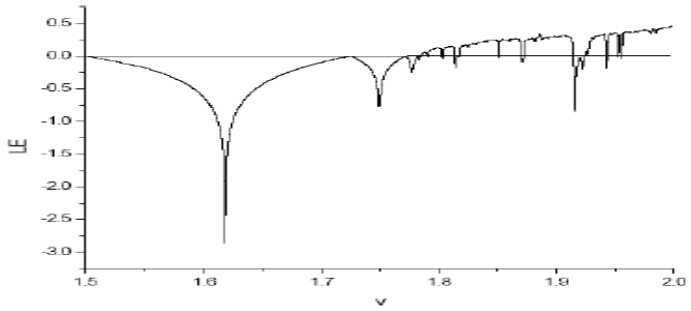


Figure 2.2: The Lyaponov exponent of the map $\varphi_\nu(x) = -2\upsilon x^2 + \left(\frac{1}{2}\upsilon - \frac{1}{2}\right)$ for $\upsilon \in [1.5, 2)$.

for all $x \in [a, b]$. Then, conditions (B1)-(B7) are satisfied. The Lyaponov exponent of the map $\varphi_\nu(x) = -2\upsilon x^2 + \left(\frac{1}{2}\upsilon - \frac{1}{2}\right)$ is shown in Figure 2.1. Here, we take $a = -\frac{1}{2}, b = \frac{1}{2}$ and $\upsilon = \lambda \in [1.5, 2)$.

■

In this case, this Lyaponov exponent is strictly positive in a wide range of the bifurcation parameter $\upsilon$.

## 2.2 Chaos in a minimal 2-D quadratic map

In this section, We've described a plane's minimal discrete quadratic chaotic map. This map's intricate dynamical characteristics, such as fixed points, bifurcations, dynamical behavior, dimension, and basin boundaries, were examined. The map is ideal for more researchs since it is filled with interesting dynamical behaviors.
The Hénom map [12] given by

$$h(x, y) = \begin{pmatrix} 1 - ax^2 + by \\ x \end{pmatrix} \tag{2.2}$$

has been widely studied because it is the simplest example of a dissipative map with chaotic solutions. It has a single quadratic nonlinearity and an area contraction that depends only on $b$ and is thus constant over the orbit in tha $ab$-plane. It can also be written as a one dimensional time-delayed map:

$$x_{n+1} = 1 - ax_n^2 + bx_{n-1} \tag{2.3}$$

Here we analyse an equally simple two-dimensional quadratic map given by

$$f(x, y) = \begin{pmatrix} 1 - ay^2 + bx \\ x \end{pmatrix} \tag{2,4}$$

where $a$ and $b$ are bifurcation parameters. Equation (2.4) is an interesting minimal system, similar to the Hénom map, but with the time delay in the non-linear rather than the linear term as evidence by writing it in the time-delayed form:

$$x_{n+1} = 1 - ax_{n-1}^2 + bx_n \tag{2.5}$$

Despite its apparent similarity and simplicity, it differs from the Hénom map in that it has a nonuniform dissipation, a more rich and varied route to chaos, and a much wider variety of attractors. The map (2.4) has attractors covering the entire range of dimensions from 1 to 2 with basin of attraction that are often much more complicated than for the Hénom map. These systems are special cases of general 2-D quadratic maps. This system is differs from other well-mnown 2-D maps such as the delayed logistic map [13] given by

$$g(x,y) = \begin{pmatrix} ax(1-y) \\ x \end{pmatrix} \tag{2.6}$$

Equation (2,4) is not topologically aquivalent to equation (2.6).

### 2.2.1 Fixed points and their stability

The Jacobian matrix of the map (2.4) is

$$J(x,y) = \begin{pmatrix} b & -2ay \\ 1 & 0 \end{pmatrix}$$

and its characteristic polynamials for a fixed point $(x,x)$ is given by

$$\lambda^2 - b\lambda + 2ax = 0 \tag{2.7}$$

The local stability of the two equilibria is studied by evaluating the roots of equation (2.7). Hence if $a \geq -\left((-b+1)/2\right)^2$, then the map (2.4) has two fixed points:

$$\begin{cases} P_1 = \left(\frac{b-1-\sqrt{4a-2b+b^2+1}}{2a}, \frac{b-1-\sqrt{4a-2b+b^2+1}}{2a}\right) \\ P_2 = \left(\frac{b-1+\sqrt{4a-2b+b^2+1}}{2a}, \frac{b-1+\sqrt{4a-2b+b^2+1}}{2a}\right) \end{cases}$$

whereas if $a < -\left((-b+1)/2\right)^2$, then the map (2.4) has no fixed point.
$P_1$ is unstable in the following cases:

1. $a \geq -\left((-b+1)/2\right)^2, b < 0.$

2. $a \geq -\left((-b+1)/2\right)^2, a > (1/2)\,b + (3/4)\,b^2 - (1/4), b > 0.$

$P_1$ is a saddle point in the following case:

1. $a \geq -\left((-b+1)/2\right)^2, a < (1/2)\,b + (3/4)\,b^2 - (1/4), b > 0.$

On the other hand, $P_2$ is unstable in the following cases:

1. $a \geq -\left((-b+1)/2\right)^2, a > (1/8)\,b^2 - (1/8)\,b^3 + (1/64)\,b^4, b \geq 2.$

2. $a \geq -\left((-b+1)/2\right)^2, a > -(1/2)\,b + (3/4), b < 2.$

3. $a \geq -\left((-b+1)/2\right)^2, a \leq (1/8)\,b^2 - (1/8)\,b^3 + (1/64)\,b^4, b > 2.$

$P_2$ is stable in the following cases:

1. $a \geq -\left((-b+1)/2\right)^2, a > (1/8)\,b^2 - (1/8)\,b^3 + (1/64)\,b^4,$
   $a \geq -\left((-b+1)/2\right)^2, a < -(1/2)\,b + (3/4), b < 2.$

2. $a \geq -\left((-b+1)/2\right)^2, a \leq (1/8)\,b^2 - (1/8)\,b^3 + (1/64)\,b^4, 0 \leq b \leq 2.$

3. $a \geq -\left((-b+1)/2\right)^2, a \leq (1/8)\,b^2 - (1/8)\,b^3 + (1/64)\,b^4,$
   $a > (1/2)\,b + (3/4)\,b - (1/4), -2 < b < 0$

$P_2$ is a saddle point in the following cases:

1. $a \geq -\left((-b+1)/2\right)^2, a \leq (1/8)\,b^2 - (1/8)\,b^3 + (1/64)\,b^4,$
   $a < (1/2)\,b + (3/4)\,b^2 - (1/4), -2 \leq b < 2.$

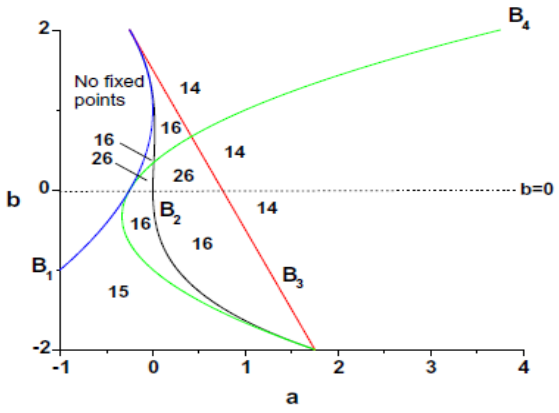


Figure 2.3: Stability of the fixed points of the map (2.4) in the ab-plane, where the numbers on the figure are as follows: 1: $P_1$ is unstable, 2: $P_1$ is a saddle, 3: $P_1$ is stable, 4: $P_2$ is unstable, 5: $P_1$ is a saddle, 6: $P_1$ is stable, and the regions $(B_i)_{1\leq i\leq 4}$ have respectively the following boundaries: $a = -\left((-b+1)/2\right)^2, a = (1/8)\,b^2 - (1/8)\,b^3 + (1/64)\,b^4, a = -(1/2)\,b + (3/4)\,, a = (1/2)\,b + (3/4)\,b^2 - (1/4)\,.$

A shematic representation of these results is given in Figure 2.3, where the regions $(B_i)_{1\leq i\leq 4}$ have respectively the following boundaries:

$$\begin{aligned} a &= -\left((-b+1)/2\right)^2, a = (1/8)\,b^2 - (1/8)\,b^3 + (1/64)\,b^4 \\ a &= -(1/2)\,b + (3/4)\,, a = (1/2)\,b + (3/4)\,b^2 - (1/4)\,. \end{aligned}$$

### 2.2.2 Numerical Computations

**Observation of chaotic attractors:** For the system (2.4) the values of $a$ and $b$ that maximize the largest Lyaponov exponent with $a = 1$ and with $b = 1$ are as follows:

1. For $a = 1$, one has $b = 0.675$ and Lyaponov exponents (base-$e$) is $0.007595$
2. For $b = 1$, one has $a = 0.59948$ and Lyaponov exponents are $0.091912$ and $-0.074313$. The corresponding chaotic attractor are shown respectively in Figure 2.4. (b) and (c) along with their basins of attraction in white. Note that the basin boundary nearly touches the attractor for these cases and is apparently a fractal for the case (c) in Figure 2.4.

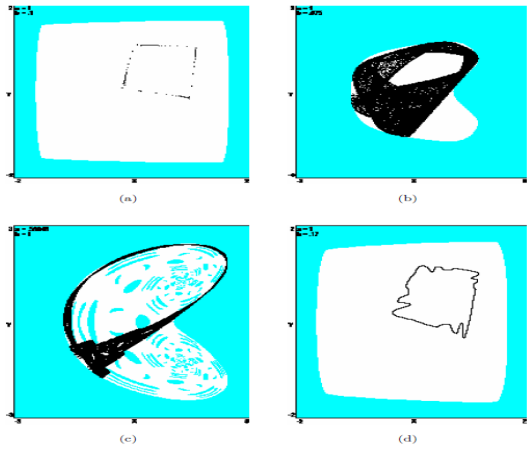

Figure 2.4: (a) A period orbit of the map (2.4) with its basin of attraction (white) obtained for $a = 1$ and $b = 0.1$. (b) The chaotic attractor with its basin of attraction (white) for $a = 1$ and $b = 0.675$. (c) Another chaotic attractor with its basin of attraction (white) for $a = 0.59948$ and $b = 1$. (d) A quasi-periodic orbit with its basin of attraction (white) for $a = 1$ and $b = 0.17$.

**Route to chaos:**

1. It is well known that the Hénom map typically undergoes a period-doubling route to chaos as the parameters are varied.

2. The Lozi map [14] has no period-doubling route, but rather it goes directly from a border-collision bifurcation developed from a stable period orbit [15;16].

3. The chaotic attractor given in [17] is obtained from a border-collision period-doubling bifurcation scenario. This scenario involves a sequence of pairs of bifurcations, whereby each pair consists of a border-collision bifurcation and a potchfork bifurcation.

4. The minimal quadratic chaotic attractor (2.4) results from a quasi-periodic route to chaos as shown in Figure 2.5.

Thus, the three chaotic systems go via different and distinguishable routes to chaos.
**Dynamical behaviors with parameter variation:** The dynamical behaviors of the map (2.4) are investigated numerically.

1. Figure 2.6 shows regions of unbounded (white), fixed point (gray), periodic (blue), quasi-periodic (green), and chaotic (red) solutions in the ab-plane for the map (2.4), where we use $|LE| < 0.0001$ as the crirterion for quasi-periodic orbits with $10^6$ iterations for each point.

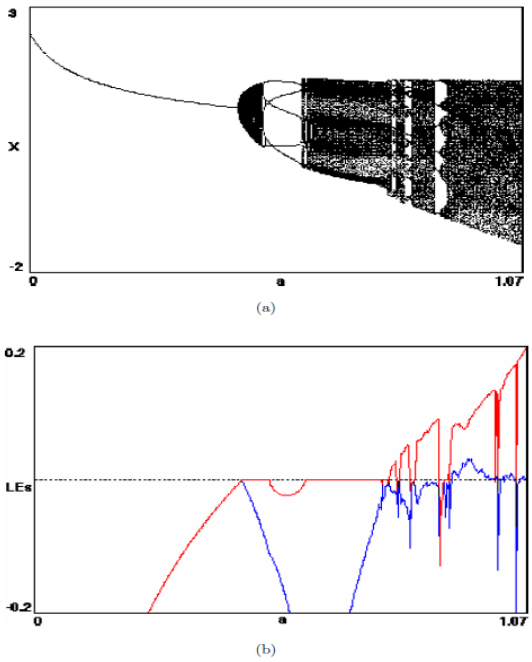


Figure 2.5: (a) The quasi-periodic route to chaos for the map (2.4) obtained for $b = 0.6$ and $0 < a \leq 1.07$. (b) Variation of the Lyaponov exponents of map (2.4) versus the parameter $0 < a \leq 1.07$ with $b = 0.6$.

2. For comparison, Figure 2.7 shows a similar plot for the Hénom map [18].

3. There are values for which both Lyaponov exponents are positive as shown in Figure 2.5. 3(b) and 6(b). indicating hyperchaos.

4. Since the map (2.4) is not everywhere dissipative, its attractor can have a dimension equal to or even greater than $2.0$ by virtue of the folding afforder by the quadratic nonlinearity.

5. The correlation dimension was calculated using the extraplation method of Sprott and Rowlands (2001) [19], and the results are ploted in Figure 2.9 for the map (2.4) with $a = 1$ and $b = 0.675$ where the Lyaponov exponents are $0.171496$ and $0.007595$. The correlation dimension is approximately constant with a value of about $1.87$ for all embeddings greater than $1$.

6. Figure 2.10 shows the regions of the $ab$-plane where the system is dissipative and bounded (in black) and where it is dissipative but area-expanding (in white) as determined from the sign of the numerical average of $\log|2ay|$ over the orbit on the attractor.

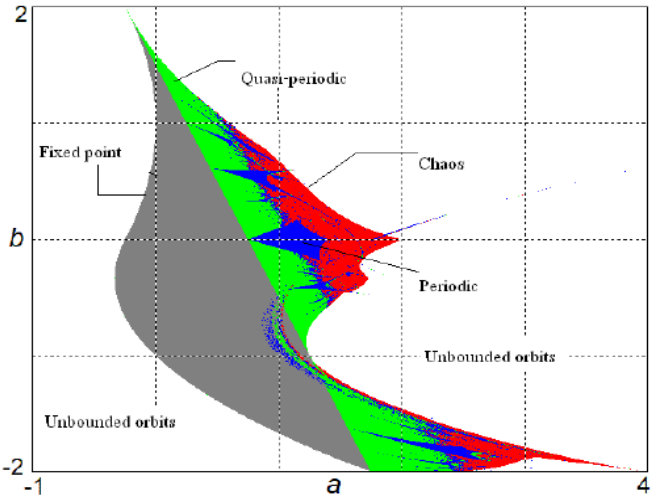


Figure 2.6: Regions of dynamical behaviors in the $ab$-plane for the map (2.4)

7. Figure 2.11 was obtained by using $200$ different random initial conditions and looking for cases where the distribution of the average value of $x$ on the attractor is bimodal.

## 2.3 Chaos in a simple $2$-D rational discrete mapping

This section present a **simple rational chaotic map** along some of its dynamical properties. In [20] the following new 1-D discrete iterative system with a rational fraction was discovered in a study of evolutionary algorithms:

$$g(x) = \frac{1}{0.1 + x^2} - ax, \tag{2.8}$$

where $a$ is a parameter, The map (2.8) describes different random evolutionary processes, and it is much more complicated than the logistic system. In [21] an extended version of the former one-dimensional discrete chaotic system given in [20] to two-dimensions is given as follows:

$$h(x, y) = \begin{pmatrix} \frac{1}{0.1+x^2} - ay \\ \frac{1}{0.1+y^2} + bx \end{pmatrix}, \tag{2.9}$$

where $a$ and $b$ are parameters. The map (2.9) has more complicated dynamical behavior than the one-dimensional map (2.8). Based on these studied in [20, 21], a new and very simple 2-D map, characterized by the existence of only one rational fraction with no vanishing denominator is constructed and is given by:

$$f(x, y) = \begin{pmatrix} \frac{-ax}{1+y^2} \\ x + by \end{pmatrix}, \tag{2.10}$$

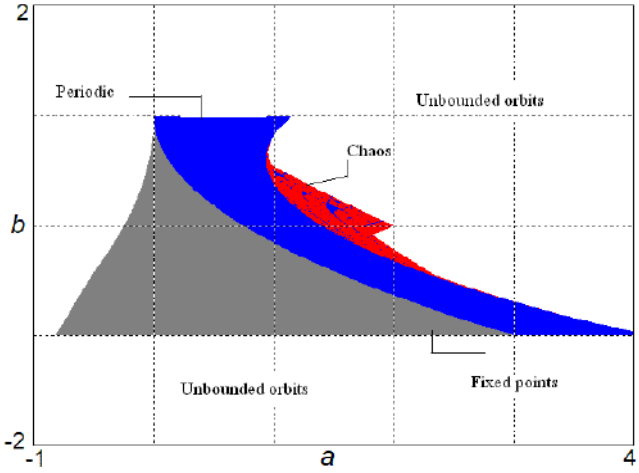


Figure 2.7: Regions of dynamical behaviors in the $ab$-plane for the Hénom map.

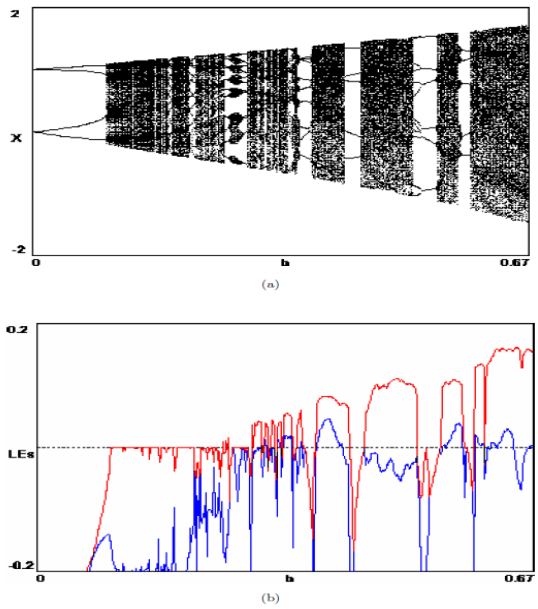


Figure 2.8: (a) The bifurcation diagram for the map (2.4) obtained for $a = 1.0$ and $0 < b \leq 67$. (b) Variation of the Lyaponov exponents of map (2.4) versus the parameter $0 < b \leq 0.67$, with $a = 1$.

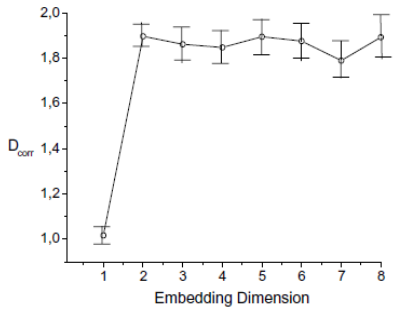


Figure 2.9: Correlation dimension versus embedding dimension for the map (2.4) with $a = 1$ and $b = 0.675$.

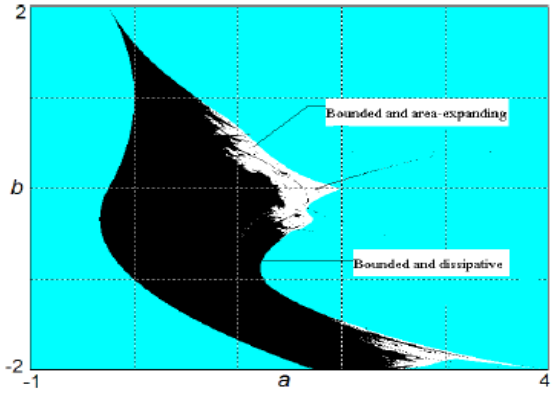


Figure 2.10: The sign of the average of $\log|2ay|$ over the orbit on the attractors of the system (2.4) in the ab-plane defines the regions of net expansion and contraction.

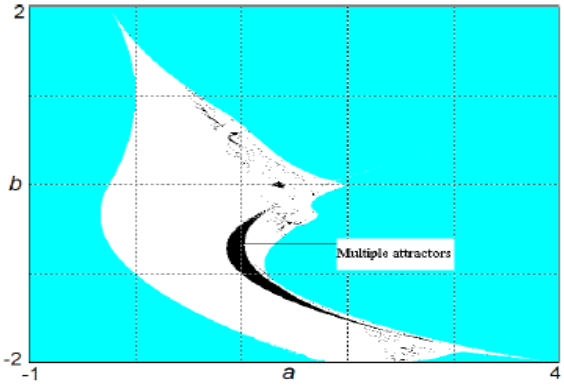


Figure 2.11: The regions of $ab-$space for multiple attractors.

where $a$ and $b$ are bifurcation parameters. First, the new map (2.10) is algebraically simpler but with more complicated behavior than map (2.9), and second, it produces several new chaotic attractors obtained via the quasi-periodic route to chaos. The essential motivation for this work is to provide a basic analysis of $f$ and to give a detailed study of its dynamics. Some basic dynamical behaviors of map (2.10) are investigated here by both theoretical analysis and numerical simulation. Possibly, this is the first simple rational map whose fraction has no vanishing denominator that gives chaotic attractors via a quasi-periodic route to chaos

**Some basic properties:** The chaotic attractors described by map (2.10) have several important properties such as:

1. The map (2.10) is defined for all points in the plane.
2. The associated function $f(x,y)$ of the map (2.10) is of class $C^{\infty}(\mathbb{R}^2)$, and it has no vanishing denominator.
3. The new chaotic map (2.10) is symmetric under the coordinate transformation $(x,y) \rightarrow (-x,-y)$, and this transformation persists for all values of the map parameters.

Briefly, the fixed points of map (2.10) are the real solutions of the equations $\frac{-ax}{1+y^2} = x$ and $x+by = y$. Assume in this paper that $-1 \leq a \leq 4$. Then if $b \neq 1$, the only fixed point of the map (2.10) is $P = (0,0)$, and if $b = 1$, then the $y-$axis is invariant by iteration of the map $f$. The Jacobian matrix of map (2.10) evaluated at a point $(x,y)$ is given by:

$$Df(x,y) = \begin{pmatrix} \frac{-a}{1+y^2} & \frac{2axy}{(1+y^2)^2} \\ 1 & b \end{pmatrix}, \tag{2.11}$$

and at the fixed point $p = (0,0)$, the Jacobian matrix is given by

$$Df(x,y) = \begin{pmatrix} -a & 0 \\ 1 & b \end{pmatrix},$$

The local stability of $P$ is studied by evaluating the eigenvalues of the Jacobian $Df(P)$. The eigenvalues of $Df(P)$ are: $\lambda_1 = -a$ and $\lambda_2 = b$. Then one has the following results:

1. If $|a| < 1$ and $|b| < 1$, then $P$ is asymptotically stable.
2. If $|a| > 1$ or $|b| > 1$, then $P$ is an unstable fixed point.

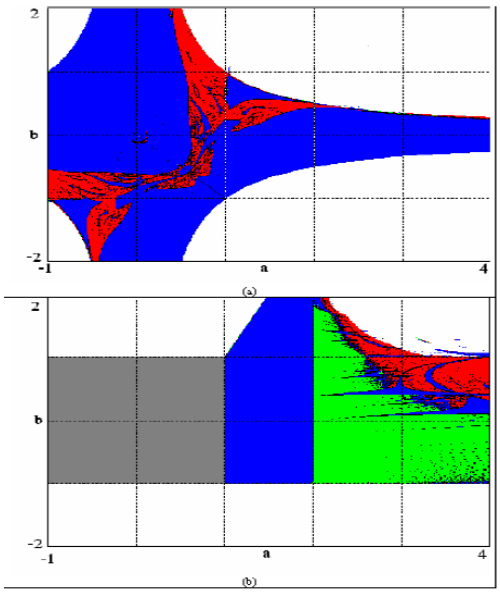


Figure 2.12: (a) Regions of dynamical behaviors in the ab-plane for the rational map (2.10). (b) Regions of dynamical behaviors in the ab-plane for the rational

3. If $|a| < 1$ and $|b| > 1$, or $|a| > 1$ and $|b| < 1$, then $P$ is saddle point.

4. If $|a| = 1$ or $|b| = 1$, then $P$ is a non-hyperbolic fixed point.

**Numerical simulations**There are several possible ways for a discrete dynamical system to make a transition from regular behavior to chaos. Bifurcation diagrams display these routes and allow one to identify the chaotic regions in $ab$-space from which the chaotic attractors can be determined. In [21] the chaotic attractors are obtained via a period-doubling bifurcation route to chaos as shown in Figure 2.12 (a) while Figure 2.12 (b) shows regions of unbounded (white), fixed point (gray), periodic (blue), quasi-periodic (green), and chaotic (red) solutions in the $ab$-plane for the map (2.10).
If we fix parameter $b = 0.6$ and vary $-1 \leq a \leq 4$, the map (2.10) exhibits the following dynamical behaviors as shown in Figure 2.13 (a):

1. In the interval $-1 \leq a \leq 1$, the map (2.10) converges to the fixed point $(0, 0)$.

2. For $1 < a \leq 2$, as shown in Figure 2.14 (a) it converges to a period-2 attractor followed by a quasi-periodic orbit for $2 < a \leq 3$.

3. In the interval $3 < a \leq 4$, it converges to a chaotic attractor shown in Figure 2.14(b) via a quasi-periodic route to chaos except for a number of periodic windows.

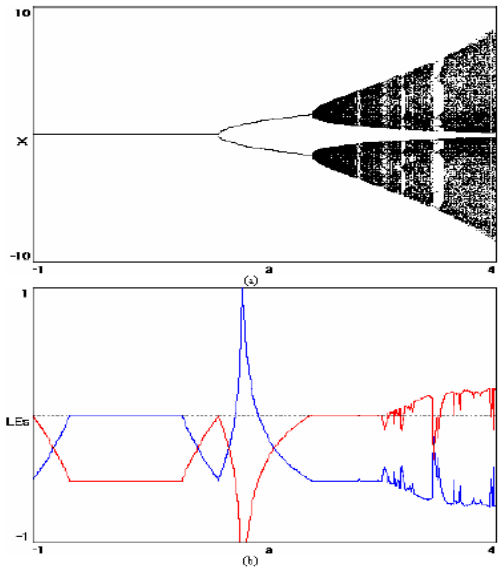


Figure 2.13: (a) The quasi-periodic route to chaos for the map (2.10) obtained for $b = 0.6$ and $-1 < a \leq 4$. (b) Variation of the Lyapunov exponents of map (2.10) versus the parameter $-1 < a \leq 4$ with $b = 0.6$.

4. We remark the appearence of a singularity in the LEs at $a = 1.25$, and $b = 0.6$.

5. The map (2.10) has dissipative orbits for the regions shown in black in Figure 2.15 and area-expanding orbits for the regions shown in white.

6. There are also regions of hyperchaos, for example at $a = 2.6$, and $b = 1.2$.

7. It is well known that basin boundaries arise in dissipative dynamical systems when two or more attractors are present, the sets that separate different basins are called the basin boundaries. For the map (2.10) we have calculated the attractors and their basins of attraction on a grid in ab-space where the system is chaotic, Figure 2.16 and 2.14 show some of a wide variety of possible attractors. Also, most of the basin boundaries are smooth, and we note that there are basins of attraction for $b > 1$, as shown in Figure 2.16 (a), but evidently none for $b < 1$.

8. There are some regular and chaotic regions in $ab$-space where two coexisting attractors apparently occur as shown in the black region of Figure 2.17.

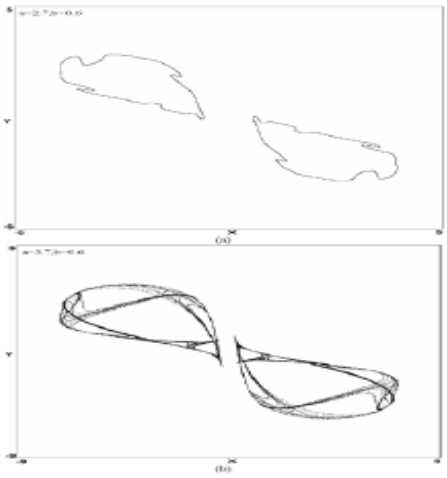

Figure 2.14: Attractors of the map (2.10) (a) Quasi-periodic orbit for $a = 2.7, b = 0.6$. (b) Chaotic orbit for $a = 3.7, b = 0.6$.

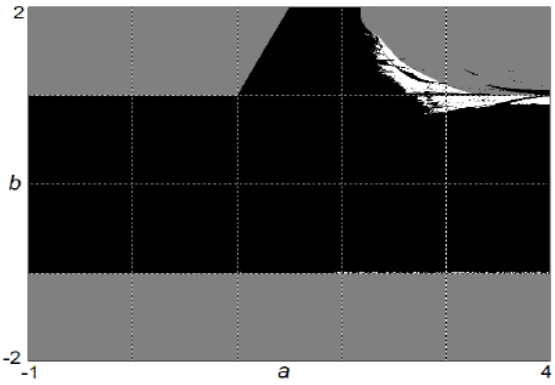


Figure 2.15: The sign of the average of $\log \left| \frac{ab+2axy+abh^2}{(y^2+1)^2} \right|$ over the orbit on the attractors of the system (2.10) in the ab-plane defines the regions of net expansion and contraction.

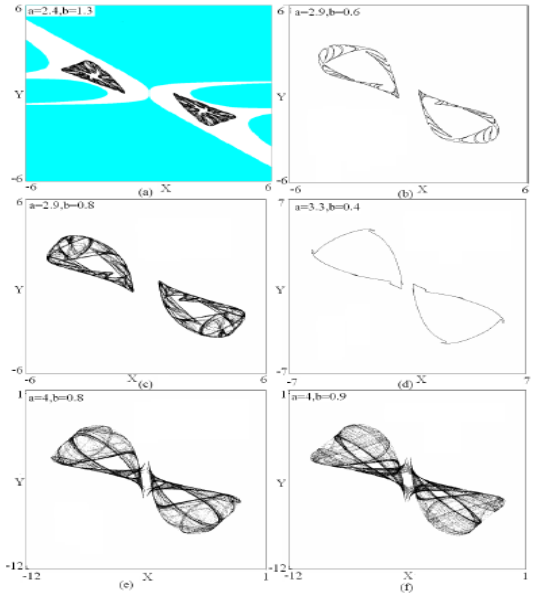


Figure 2.16: Attractors of the map (2.10) with (a) $a = 2.4, b = 1.3$,(b) $a = 2.9, b = 0.6$,(c) $a = 2.9$, $b = 0.8$,(d) $a = 3.3, b = 0.4$,(e) $a = 4$, $b = 0.8$,(f) $a = 4, b = 0.9$.

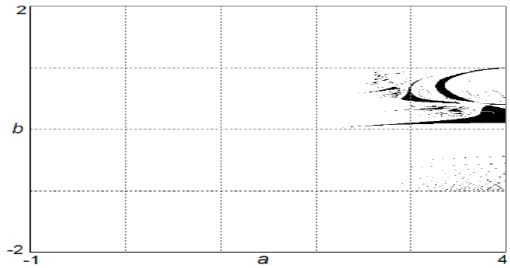


Figure 2.17: The regions of ab-space with multiple attractors for the map (2.10), obtained by using $200$ different random initial conditions and looking for cases where the distribution of the average value of $x$ on the attractor is bimodal.

# Chapter 3

# Chaos in some 2-D piecewise Zeraoulia-Sprott mappings

This chapter examines the finding of chaos in 2-D piecewise Zeraouilia-Sprott mappings. By employing mathematical analysis and numerical simulations, the research investigates the presence of chaotic behavior characterized by sensitive dependence on initial conditions, the presence of strange attractors, and irregular dynamics. Furthermore, the impact of key parameters on the chaotic dynamics is explored, revealing bifurcation scenarios and transitions between different dynamical regimes. This findings contribute to the understanding of chaos theory and its implications in various scientific domains.

## 3.1 Chaos in a discrete hyperchaotic double scroll

This section have described a simple 2-D discrete piecewise linear chaotic map that is capable of generating a hyperchaotic double scroll attractor. it calls **the discrete hyperchaotic double scroll**. It has the same non-linearity as used in the well known **Chua circuit**. It is well known that if two or more Lyaponov exponents of a dynamical system are positive throughout of parameter space, then the resulting attractors are hyperchaotic. The importance of these attractors is that they are less regular and are seemingly **almost full** in space. On the other hand, the attractors generated by Chua's circuit [22] given by

$$\begin{aligned} x' &= \alpha\left(y - h\left(x\right)\right) \\ y' &= x - y + z \\ z' &= -\beta y \end{aligned}$$

are associated with saddle-focus homoclinic loops are not hyperchaotic.
where $h(x) = \frac{2m_1x+(m_0-m_1)(|x+1|-|x-1|)}{2}$. The double scroll attractor for this case is shown in Figure 3.1.

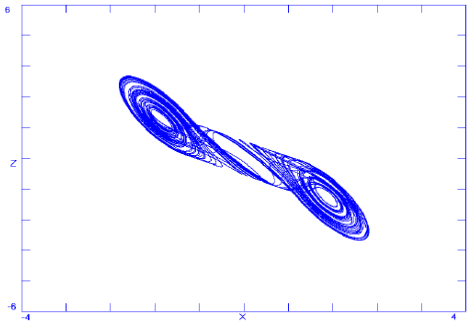

Figure 3.1: The classic double scroll attractor obtained for $\alpha = 9.35, \beta = 14.79, m_0 = -\frac{1}{7}, m_1 = \frac{2}{7}$

The double scroll is more complex than the Lorenz-type and the hyperbolic attractors. The circuit realizations of low-dimensional maps is simpler than with high-dimensional continuous systems. For this reason, we present a discrete version of Chua's circuit attractor governed by a simple 2-D piecewise linear map that is capable of producing hyperchaotic attractors with the same shape as the classic double scroll attractor, which is not hyperchaotic.

### 3.1.1 A formula for a discrete hyperchaotic double scroll map

We present the new map and show some of its basic properties. Consider the following 2-D piecewise linear map:

$$f(x,y) = \begin{pmatrix} x - ah(y) \\ bx \end{pmatrix} \tag{3.1}$$

where $a$ and $b$ are the bifurcation parameters, $h$ is given above by the characteristic function of the so-called **double scroll attractor** and $m_0$ and $m_1$ are respectively the slopes of the inner and outer sets of the original Chua circuit. Systems such as the one in (3.1) typpically have no direct application to particular physical systems, but they serve to exemplify the kinds of dynamical behaviors, such as routes to chaos, that are common in physical chaotic systems. We call it **discrete hyperchaotic double scroll** because of its similarity to the well-known Chua circuit.
Firstly, the associated function $f(x,y)$ is continuous in $\mathbb{R}^2$, but it is not differentiable at the points $(x,-1)$ and $(x,1)$ for all $x \in \mathbb{R}$. Secondly, the map (3.1) is a diffeomorphism except at points $(x,-1)$ and $(x,1)$ when $abm_1m_0 \neq 0$, since the determinant of its Jacobian is non zero if and only if $abm_0 \neq 0$ or $abm_1 \neq 0$, but it does not preserve area and it is not a reversing twist map for

all values of the systel parameters. Thirdly, the map (3.1) is symmmetric under the coordinate transformion $(x, y) \to (-x, -y)$ , and this transformation persists for all values of the system parameters. Therefor, the chaotic attractor obtained for map (3.1) is symmetric just like the classical double scroll.
Due to the shape of the vector field $f$ of the map (3.1), the plane can be devided into three linear regions denoted by:

$$\begin{aligned} R_1 &= \left\{(x, y) \in \mathbb{R}^2 / y \geq 1\right\}, \\ R_2 &= \left\{(x, y) \in \mathbb{R}^2 / \left|y\right| \leq 1\right\}, \\ R_3 &= \left\{(x, y) \in \mathbb{R}^2 / y \leq -1\right\}. \end{aligned}$$

where in each of these regions the map (3.1) is linear. However, it is easy to verify that for all values of the parameters $m_0, m_1$ such that $m_0 m_1 > 0$, the map (3.1) has a single fixed point $(0, 0)$, while if $m_0 m_1 < 0$, the map (3.1) has three fixed points, and they are given by

$$\begin{aligned} P_1 &= \left(\frac{m_1 - m_0}{b m_1}, \frac{m_1 - m_0}{m_1}\right), \\ P_2 &= (0, 0), \\ P_3 &= \left(\frac{m_0 - m_1}{b m_1}, \frac{m_0 - m_1}{m_1}\right). \end{aligned}$$

Obviously, the Jacobian matrix of the map (3.1) evaluated at the fixed points $P_1$ and $P_3$ is the same and given by

$$J_{1,3} = \begin{pmatrix} 1 & -abm_1 \\ 1 & 0 \end{pmatrix}$$

Therefore, the two equilibrium points $P_1$ and $P_3$ have the same stability type. The Jacobian matrix of the map (3.1) evaluated at the fixed point $P_2$ is given by

$$J_2 = \begin{pmatrix} 1 & -abm_0 \\ 1 & 0 \end{pmatrix}$$

where the local stability of these equilibria can be studied by evaluating the eigenvalues of the corresponding Jacobian matrices given by the solution of their characteristic polynomials.

### 3.1.2 The hyperchaoticity of the attractor

We give sufficient conditions for the hyperchaoticity of the discrete hyperchaotic double scroll given by the map (3.1). It is shown in [23] that if we consider a system $x_{k+1} = f(x_k), x_k \in \Omega \subset$

$\mathbb{R}^n$, such that

$$\|f'(x)\| \leq N < +\infty$$

with a smallest eigenvalue of $f'(x)^T f'(x)$ that satisfies

$$\lambda_{\min}\left(f'(x)^T (f'(x))\right) \geq \theta > 0,$$

where $N^2 \geq \theta$, then for any $x_0 \in \Omega$, all the Lyaponov exponents at $x_0$ are located inside $\left[\frac{\ln\theta}{2}, \ln N\right]$, that is,

$$\frac{\ln\theta}{2} \leq l_i \leq \ln N, \qquad i = 1, 2, ..., n$$

where $l_i$ are the Lyaponov exponents for the map $f$. For the map (3.1), one has that

$$\|f'(x,y)\| = \begin{cases} \sqrt{\frac{b^2+a^2m_1^2+\sqrt{2b^2+b^4+2a^2m_1^2+a^4m_1^4-2a^2b^2m_1^2+1}+1}{2}}, & \text{if} \quad |y| \geq 1 \\ \sqrt{\frac{b^2+a^2m_0^2+\sqrt{2b^2+b^4+2a^2m_0^2+a^4m_0^4-2a^2b^2m_0^2+1}+1}{2}}, & \text{if} \quad |y| \leq 1 \end{cases} < +\infty$$

and

$$\lambda_{\min}\left(f'(x)^T f'(x)\right) = \begin{cases} \frac{b^2+a^2m_1^2-\sqrt{2b^2+b^4+2a^2m_1^2+a^4m_1^4-2a^2b^2m_1^2+1}+1}{2}, & \text{if} \quad |y| \geq 1 \\ \frac{b^2+a^2m_0^2-\sqrt{2b^2+b^4+2a^2m_0^2+a^4m_0^4-2a^2b^2m_0^2+1}+1}{2}, & \text{if} \quad |y| \leq 1 \end{cases}$$

If

$$\begin{cases} |a| > \max\left(\frac{1}{|m_1|}, \frac{1}{|m_0|}\right) \\ |b| > \max\left(\frac{|am_1|}{\sqrt{a^2m_1^2-1}}, \frac{|am_0|}{\sqrt{a^2m_0^2-1}}\right) \end{cases}$$

then both Lyaponov exponents of the map (3.1) are positive for all initial conditions $(x_0, y_0) \in \mathbb{R}^2$, and hence the corresponding attractor is hyperchaotic, Figure 3.2 shows the Lyaponov exponent spectrum for the map (3.1). The regions of hyperchaos are $-3.365 \leq a \leq 3.323$ and $-3.323 \leq a \leq 3.365$.

The discrete hyperchaotic double scroll results from a stable period-3 orbit transitioning to a fully developed chaotic regime, as shown in Figure 3.3.

This particular type of bifurcation is called a border-collision bifurcation as shown in Figure 3.4, and it is only observed scenario. For $-3.365 \leq a \leq 3.365$, the map (3.1) begins with a reverse border collision bifurcation leading to a stable period-3 orbit, and then collapses to a point that is reborn as stable period-3 orbit leading to fully developed chaos,However, it seems that the proposed map behaves in a similar way to the 4-D dynamical system given in [24], i.e., both hyperchaotic attractors are obtained by a border-collision bifurcation [25].

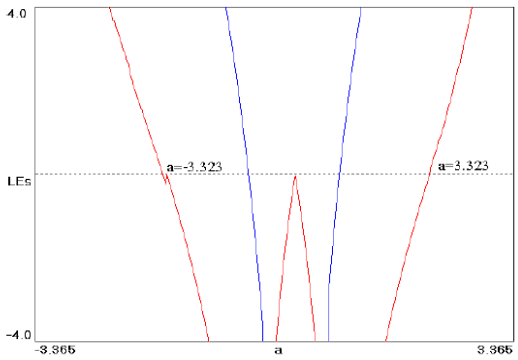


Figure 3.2: Variation of the Lyaponov exponents of the map (3.1) versus the parameter $-3.365 \leq a \leq 3.365$ with $b = 1.4$, $m_0 = -0.43$, and $m_1 = 0.41$.

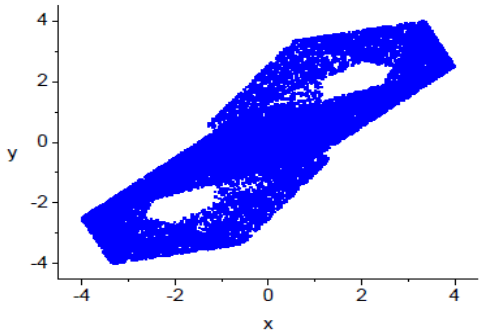


Figure 3.3: The discrete hyperchaotic double scroll attractor obtained from the map (3.1) for $a = 3.36$, $b = 1.4$, $m_0 = -0.43$, and $m_1 = 0.41$ with initial conditions $x = y = 0.1$.

Figure 3.5 shows regions in the $ab$-plane given by $(a, b) \in [-3.365, 3.365] \times [-2, 2]$ of unbounded (white), periodic orbits of period $1$ and $3$ (blue), and chaotic (including hyperchaotic attractors) (red) solutions in the ab-plane for the map (3.1), with $10^6$ iterations for each point are shown in .

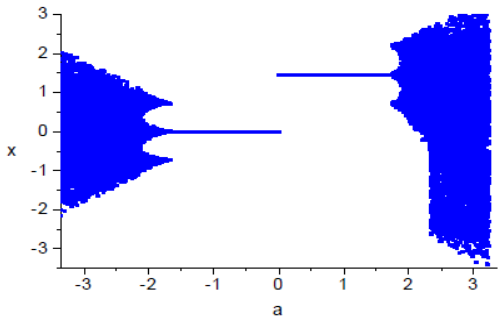


Figure 3.4: The border-collision bifurcation route to chaos of the map (3.1) versus the parameter $-3.365 \leq a \leq 3.365$ with $b = 1.4$, $m_0 = -0.43$, and $m_1 = 0.41$.

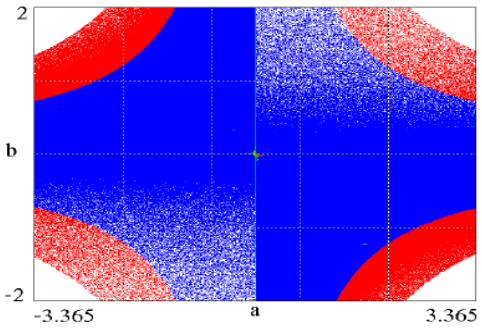


Figure 3.5: Regions of dynamical behaviors in the $ab$-plane for the map (3.1).

## Conclusion

In conclusion, this study focused on the exploration of chaos in certain Zeraouilia-Sprott mappings. The objective was to investigate the dynamical behaviors and chaotic properties exhibited by these mappings which commenced by providing a comprehensive overview of chaos theory and its relevance in various scientific disciplines. It established a theoretical foundation for understanding the chaotic phenomena observed in dynamical systems. Additionally, the study introduced the Zeraouilia-Sprott mappings, which are a class of discrete dynamical systems known for their chaotic behaviors, through rigorous mathematical analysis, numerical simulations, and graphical representations. This study revealed the presence of chaos in the Zeraouilia-Sprott mappings under investigation and the chaotic nature was identified by observing sensitive dependence on initial conditions, irregular and aperiodic behavior, and the presence of strange attractors. The examination of bifurcations diagrams also covered the emergence of complex dynamical regimes, including period-doubling cascades and intermittency. Furthermore, this research explored the influence of key parameters on the chaotic dynamics of the Zeraouilia-Sprott mappings. It was observed that slight variations in the parameter values could lead to significant changes in the system's behavior, resulting in transitions from regular to chaotic motions and contribute to the understanding of chaos theory and its manifestation. The identification and characterization of chaotic behavior in these mappings expand the existing knowledge of discrete dynamical systems and their applications. The results also have implications in various fields such as physics, biology, and engineering, where chaos theory has diverse applications. Overall, this memory of the master's degree project demonstrates the complexity and richness of chaos in some selected Zeraouilia-Sprott mappings. The research outcomes provide a valuable insights into the dynamics of these mappings and the groundwork for further investigations in the realm of chaos theory and its practical implications.

# Bibliography


[1] E. Zeraoulia, Chaotifying one-dimensional discrete mappings using $S$-unimodality and Collet-Eckmann condition, International Journal of Bifurcations and Chaos, **29** (4), 1950050, 2019.

[2] E. Zeraoulia and J. C. Sprott, A minimal 2-D quadratic map with quasi-periodic route to chaos, International Journal of Bifurcations and Chaos, **18** (5), 1567-1577, 2008.

[3] E. Zeraoulia, *On the dynamics of a new simple 2-D rational discrete mapping,* International Journal of Bifurcations and Chaos, **21** (1), 155-160, 2011.

[4] E. Zeraoulia and J. C. Sprott, *The discrete hyperchaotic double scroll*. International Journal of Bifurcations and Chaos, **19** (3), 1023-1027, 2009.

[5] M. I. Feigin, *Doubling of the oscillation period with $C$-bifurcations in piecewise continuous systems*, Prikl, Mat, Meh, **34**, 861-869, 1970.

[6] H. E. Nusse and J. A. Yorke, *Border-collision bifurcations including "period two to period three" for piecewise smooth systems*, Phys, D, **57** (1-2), 39-57, 1992.

[7] C. H. Wong, *Border collision bifurcations in piecewise smooth systems*, A thesis for the degree of Doctor of Philosophy, University of Manchester, 2011.

[8] S. Banerjee and C. Grebogi, *Border collision bifurcations in two-dimensional piecewise smooth maps*, Phys, Rev, E, **59** (4), 4052-4061, 1999.

[9] S. Banerjee, M. S. Karthik, G. Yuan, and J. A. Yorke, *Bifurcations in one-dimensional piecewise smooth maps– theory and applications in switching circuits,* IEEE Trans, Circuits Systems I Fund. Theory Appl, **47** (3), 389-394, 2000.

[10] E. Zeraoulia, *Dynamical systems*, Theory and Applications, Science Publishers, 2018.

[11] D. Singer, *Stable orbits and bifurcation of maps of the interval*, SIAM J. Appl. Math. **35**, 260–267, 1978.

[12] M. Hénom, *A two dimensional mapping with a strange attractor,* Commun. Math, Phys. **50**, 69-77, 1976.

[13] D. G. Aronson, M. A. Chory, G. R. Hall, R. P. McGe- hee, *Bifurcations from an invariant cir-cle for two-parameter families of maps of the plane: A computer-assisted study*, Commun. Math. Phys. **83**, 303–354, 1982.

[14] R. Lozi, *Un attracteur étrange du type attracteur de Hénon*, J. Physique. Col loque C5, Supplément au n° 8, **39**, 9–10, 1978.

[15] Y. Cao, Z. Liu, *Orientation-preserving Lozi map*, Chaos Solit. Fract.**9**, 1857–1863, 1998.

[16] M. A. Aziz-Alaoui, C. Robert, C. Grebogi, *Dynamics of a Hénon–Lozi map*, Chaos Solit. Fract. **12**, 2323–2341, 2001.

[17] E. Zeraoulia, *A new chaotic attractor from 2-D discrete mapping via border-collision period doubling scenario*, Discr. Dyn. Nature Soci. **9**, 235–238, 2005.

[18] J. C. Sprott, Chaos and Time-Series Analysis, Oxford University Press, 2003.

[19] J. C. Sprott, G. Rowlands, *Improved correlation dimension calculation*, Int. J. Bifurcation and Chaos **11**, 1865–1880, 2001.

[20] J. A. Lu, X. Wu, J. Lu, L. Kang, *A new discrete chaotic system with rational fraction and its dynamical behaviors,* Chaos, Solitons & Fractals **22,** 311-319, 2004.

[21] L. Chang, J. Lu, X. Deng, *A new two-dimensional discrete chaotic system with rational fraction and its tracking and synchronization,* Chaos, Solitons & Fractals **24**, 1135-1143, 2005.

[22] L. O. Chua, M. Komuro, T. Matsumoto, *The double scroll family*, Part I and II, IEEE Trans. Circuits. Syst. CAS-33, 1073—1118, 1986.

[23] C. Li, G. Chen, *Estimating the Lyapunov exponents of discrete systems*, Chaos. **14** (2), 343—346, 2004.

[24] K. Thamilmaran, M. Lakshmanan, A. Venkatesan, *Hyperchaos in a Modified Canonical Chua's Circuit*, Int. J. Bifurcation and Chaos. **14** (1), 221—244, 2004.

[25] S. Banerjee, C. Grebogi, *Border collision bifurcations in two-dimensional piecewise smooth maps*, Phys. Rev. E. **59** (4), 4052—4061, 1999.

[26] M. Burger, R. Fetecau, Y. Huang, *Stationary states and asymptotic behavior of aggregation models with nonlinear local repulsion*. SIAM Journal on Applied Dynamical Systems, **13**(1), 397-424, 2014.